https://doi.org/10.5194/egusphere-2025-1351
Preprint. Discussion started: 17 April 2025

Response and recovery of a *Sphagnum* peatland from long-term human-induced alkalinisation

Luke Oliver Andrews [a, b], *Katarzyna Marcisz* [a], *Piotr Kołaczek* [a], *Leeli Amon* [c], *Siim Veski* [c], *Atko Heinsalu* [c], *Normunds Stivrins* [d], *Mariusz Bąk* [a], *Marco A. Aquino-Lopez* [e], *Anna Cwanek* [f], *Edyta Łokas* [g], *Monika Karpińska-Kołaczek* [a], *Sambor Czerwiński* [a, h], *Michał Słowiński* [i], *Mariusz Lamentowicz* [a]

Corresponding author: Luke Andrews, l.o.andrews@ljmu.ac.uk, ORCID ID: https://orcid.org/0000-0002-8494-4791

a. *Climate Change Ecology Research Unit, Adam Mickiewicz University, Poznań, Poland.*
b. *School of Biological and Geographical Studies, Liverpool John Moores, Liverpool, UK (present address).*
c. *Department of Geology, Tallinn University of Technology, Tallinn, Estonia.*
d. *University of Latvia, Riga, Latvia.*
e. *Department of Geography, University of Cambridge, Cambridge, UK.*
f. *Department of Mass Spectrometry, Institute of Nuclear Physics Polish Academy of Sciences, Krakow, Poland.*
g. *Institute of Nuclear Physics, Polish Academy of Sciences, Warsaw, Poland.*
h. *Department of Geomorphology and Quaternary Geology, University of Gdańsk, Bażyńskiego 4, 80-309, Gdansk, Poland*
i. *Institute of Geography and Spatial Organization, Polish Academy of Sciences, Warsaw, Poland.*

Keywords: Alkalinisation, Carbon, Vegetation, Palaeoecology, Multi-proxy, Peatland.

https://doi.org/10.5194/egusphere-2025-1351
Preprint. Discussion started: 17 April 2025

Abstract

Northern peatlands are significant terrestrial carbon stores but are increasingly threatened by human activities. Ombrotrophic peatlands, being naturally acidic, are particularly vulnerable to alkaline pollution. Despite their importance, the effects of alkalinisation on peatlands remain insufficiently studied. In Estonia, alkaline pollution from a cement industry and oil shale power plant emissions have degraded several peatlands since the 19th century. Although some sites have recovered in recent decades, more severely impacted areas remain in poor condition.

We investigated the effects of alkalinisation on Varudi peatland, a forested site in northeast Estonia, which was exposed to 125 years of alkaline emissions from a nearby cement factory. Using a multi-proxy, high-resolution palaeoecological approach combined with a precise and reliable age-depth model, we reconstructed changes in environmental, chemical, botanical, and hydrological conditions over the past millennium. Our findings revealed three successional phases: during the mid-12th century CE, land clearance and increased mineral deposition caused the site to transition from a bog to a poor fen phase between approximately 1250-1570 CE; and while the cement factory operated without efficient filters, the site became a pine-dominated fen between 1871-1995.

After the installation of filters in 1996, peatland pH returned to pre-disturbance levels, and some recovery was observed. However, the site remains degraded. Our results indicate that alkalinisation significantly disrupts peatland functioning, reducing carbon storage and altering vegetation communities. These effects can persist for decades even after the source of contamination is removed, underscoring the need for more comprehensive monitoring of peatlands impacted by alkaline pollution globally.

https://doi.org/10.5194/egusphere-2025-1351
Preprint. Discussion started: 17 April 2025

1. Introduction

Despite only covering c. 3% of the Earth's surface, northern peatlands contain >500 gigatonnes of carbon (Bridgham *et al.,* 2008; Yu *et al.,* 2010; Yu, 2012). Their capacity to accumulate and store carbon results from the waterlogged and acidic nature of their soils (Clymo *et al.,* 1998). These conditions preserve organic material, which accumulates and may be stored indefinitely (Harenda *et al.,* 2018). Since their initiation, peatlands have slowly removed carbon from the atmosphere, imparting a weak but persistent cooling effect upon global climate over millennial timescales (Frolking *et al.,* 2006).

Despite being recognised as a valuable tool for climate change mitigation, peatlands still receive little protection, regionally or nationally (Rawlins and Morris, 2010). As of 2018, approximately 10% of the remaining peatlands worldwide are in a degraded state (Leifeld and Menichetti, 2018), while in Europe this rises to 25% (Tanneberger *et al*., 2021). Such disturbance can disrupt the fragile hydrological balance that maintains the carbon sink function of peatlands and may cause them to shift from sinks to sources of atmospheric carbon, exacerbating climate change (Leifeld and Menichetti, 2018).

Estonia is one of Europe's most peat-rich countries, with peatlands covering c. 22.5% of its land area (Orru and Orru, 2008). Due to this abundance, peat is a significant natural resource for Estonia, and has been heavily exploited, particularly after the Industrial Revolution (Paal *et al.,* 2010; Łuców *et al.,* 2022). The rise in anthropogenic pollution since this time has caused substantial changes in global geochemistry such that this era is informally termed 'the Anthropocene' (Fiałkiewicz-Kozieł *et al*., 2018; Waters *et al*., 2023). During this time in Estonia, emissions from industrial sources were characterised by high levels of calcium-rich particulate matter, with most of the emissions concentrated in the northeastern industrial region of the country (Liblik *et al.,* 1995; Karofeld, 1996). Ombrotrophic peat bogs, which are the dominant type of peatlands in Estonia, being naturally acidic and nutrient-poor ecosystems are particularly sensitive to alkaline atmospheric pollution (Paal *et al.,* 2010). These emissions caused significant changes in the geochemical and botanical composition of bogs adjacent to pollution sources, which resulted in dramatic increases in pore-water pH and losses of bog-specific vegetation (including *Sphagnum* mosses) near affected sites (Paal *et al.,* 2010; Vellak *et al.,* 2014). This was often followed by encroachment of *Pinus sylvestris* (Scots

https://doi.org/10.5194/egusphere-2025-1351
Preprint. Discussion started: 17 April 2025

pine) onto polluted sites alongside other species typical of nutrient-rich alkaline environments (Pensa *et al.,* 2004, 2007; Ots and Reisner, 2006; Kaasik *et al.,* 2008; Kask *et al.,* 2008).

By the 1990s, industrial emissions in Estonia began to fall, following a decline in power generation and improved filtration systems in factories (Liiv and Kaasik, 2004). Following these reductions, polluted peatland sites began to show signs of recovery, with acidic conditions and bog-specific vegetation returning (Karofeld, 1996; Kaasik *et al.,* 2008; Paal *et* al., 2010). However, in more heavily polluted sites this recovery has been slow, and the impact of past alkaline pollution persists to this day in some areas (Ots and Reisner, 2006). It remains unclear whether current levels of atmospheric pollution are sufficiently low to permit their full recovery in the future, or how long this process will take (Paal *et al.,* 2010). Despite growing concerns over alkaline pollution and its potential future effect on peatlands, particularly concerning their role as carbon reservoirs, research exploring the effects of alkalinisation upon peatland ecosystems and their subsequent recovery has been limited.

Atmospheric pollution remains a significant threat to peatland ecosystem functioning (Bobbink *et al.,* 1998; Turetsky and St Louis, 2006; Osborne *et al.,* 2024). The effects of alkaline pollution upon peatlands have been relatively overlooked relative to those of acid rain due to its effects being more localised (Vellak *et al.,* 2014; Sutton *et al.,* 2020). However, nearly two billion tonnes of alkaline residues are emitted into the atmosphere each year (Gomes *et al.,* 2016). Despite environmental standards curbing emissions in recent decades, in some areas these regulations are not consistently enforced or are merely declarative (Abril *et al.,* 2014; Ivanov *et al.,* 2018). Following global reductions in acid rain since the 1980s, the relative proportion of alkaline pollutants in airborne particulate matter has increased in UK, much of Europe, North America and China since 1986 (Turetsky and St Louis, 2006; Sutton *et al.,* 2020). Additionally, climate change may exacerbate the effects of alkaline pollution in boreal regions, as permafrost thawing may cause the expansion of areas of open water, increasing surface runoff and infiltration in some regions (Walvoord and Kurylyk, 2016). This may allow for longer contact times between surface water and carbonate bedrock, accelerating weathering and raising the pH of surface waters which may then enter peatlands in the surrounding catchment (Schindler, 1997; Osterkamp *et al.,* 2000; Lehmann *et al.,* 2023).

https://doi.org/10.5194/egusphere-2025-1351
Preprint. Discussion started: 17 April 2025

In this study, we focus on the effects of alkalinisation resulting from over 125 years of intense emissions from a nearby cement factory upon Varudi soo (bog), a formerly ombrotrophic peatland in northeastern Estonia. By employing a high-resolution, multi-proxy palaeoecological framework, we reconstruct changes in the chemical, botanical, hydrological and environmental conditions of the site over the past millennium to address the following questions:

1. What is the current state of a heavily polluted raised bog almost 30 years after the reduction in alkaline pollution?
2. How has alkaline pollution altered the ecosystem functioning of the site and how does this compare with pre-disturbance conditions?
3. To what extent has this ecosystem function recovered 30 years after removing the point source of pollution?
4. Can we identify critical transitions that can be broadly applied to assess peatland condition and recovery following alkaline pollution?

2. Methods and materials

2.1. Study area

Varudi bog (59°26'19"N, 26°35'13"E) is located in Lääne-Virumaa, northeastern Estonia, consisting of fen-bog habitats. The site is approximately 10 km south of the coast of the Gulf of Finland and Baltic Klint (Figure 1) and spans c. 12.6 km^2. The site is primarily a forested *Sphagnum* bog interspersed by numerous bog pools and hummocks, with an overstory of *Pinus sylvestris.* Varudi peatland receives 478 mm of rainfall per year, has a mean annual temperature of 7.3 °C, and prevailing winds are from the southwest and south. The underlying bedrock is composed of Cambrian and Lower Ordovician siliciclastic sedimentary rocks and Middle Ordovician limestones (Sibul *et al.,* 2017) covered with a relatively thin layer of glacial and post-glacial sediments.

https://doi.org/10.5194/egusphere-2025-1351
Preprint. Discussion started: 17 April 2025

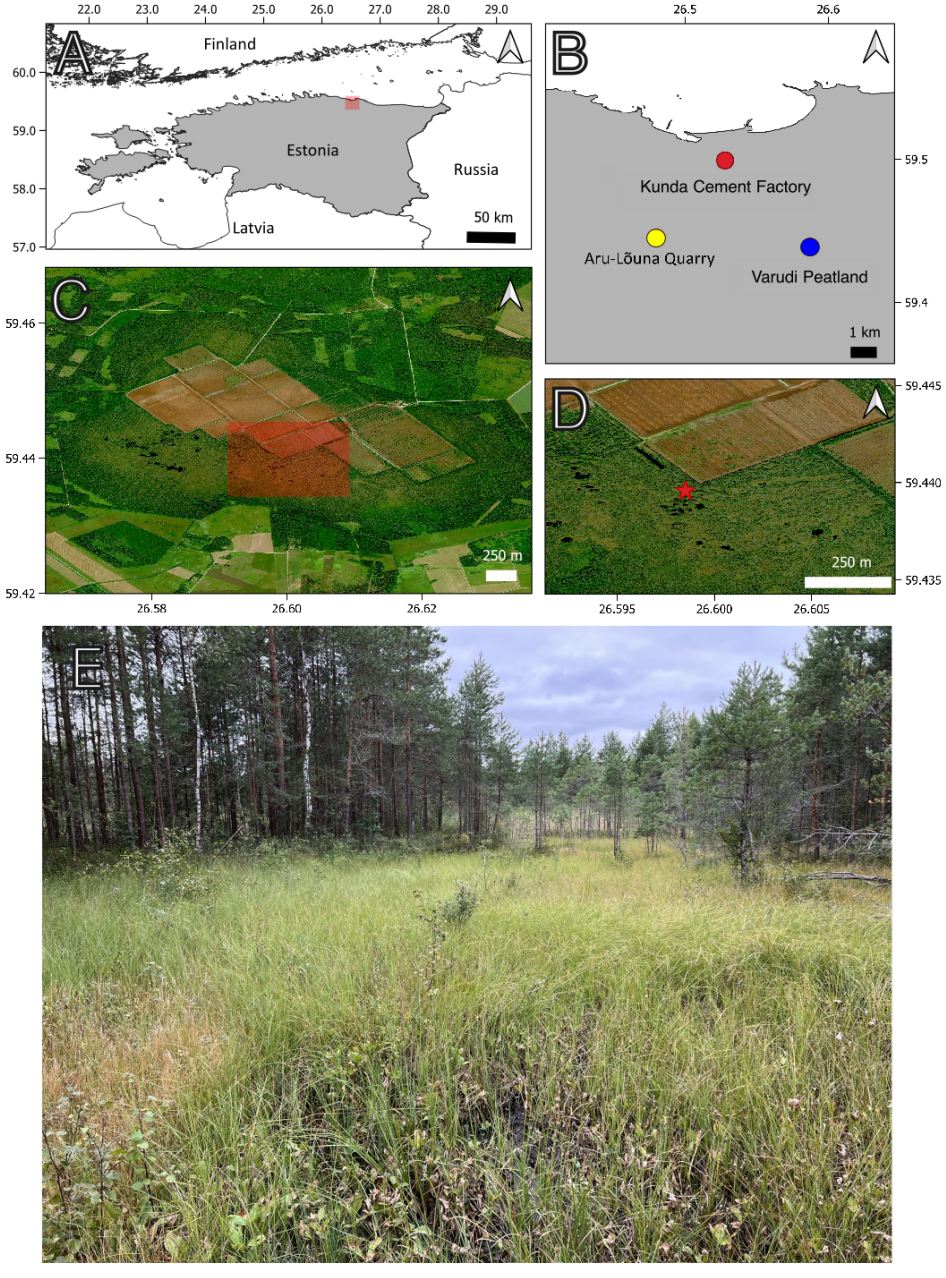

Figure 1: Map of study locations. A. Modern-day Estonia (in Gray). The red shaded square in map 1A indicates the area mapped in map 1B. B. Locations of sites relevant to this study (Kunda Cement Factory: Red, Aru-Lõuna Quarry: Yellow, Varudi peatland: Blue). C. Satellite image of Varudi bog (© Microsoft) showing the extent of peat cutting and drainage that has taken place over the past century. The red-shaded area indicates the area mapped in map 1D. D. Close-up of the location from where core VAR1 was recovered (red star). E. Coring location.

https://doi.org/10.5194/egusphere-2025-1351
Preprint. Discussion started: 17 April 2025

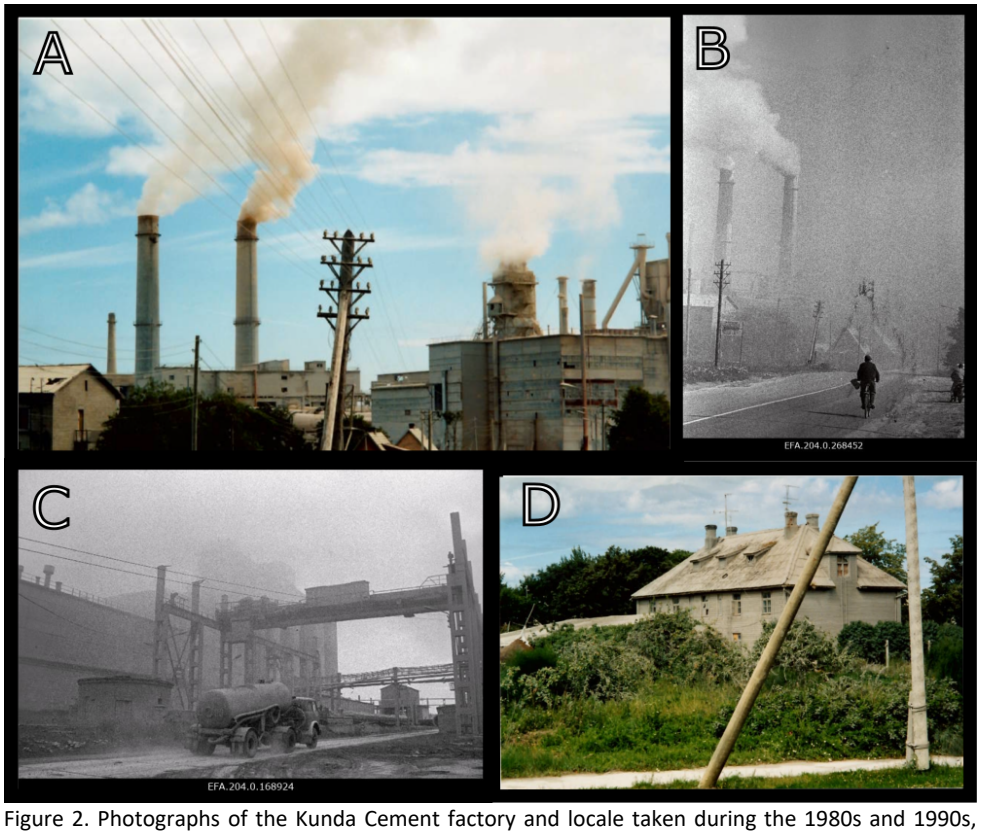

Figure 2. Photographs of the Kunda Cement factory and locale taken during the 1980s and 1990s, showing A. Cement dust emissions from the chimneys. B. Photograph of chimneys and factory surroundings. C. Photograph of the factory workings, showing substantial cement dust deposition in the surrounding area. D. Photograph showing cement dust deposition upon house near the factory. Photography by: A and D: Atko Heinsalu taken in the early 1990s; B: Estonian National Archives Photo Database (code EFA.204.0.268452) August 1994 Albert Truuväärt. C: Estonian National Archives Photo Database (code EFA.204.0.168924) August 1989 Tiit Veermäe.

Varudi was selected for study due to its proximity (7.5 km NW) to the Kunda Nordic Tsement Factory (henceforth Kunda Cement Factory) (Figures 1 and 2), which has been operational since the 1870s. During the late 1970s, cement production peaked at c. 1.2 million tonnes per year (Figure 3). The dust emissions from the cement plant have fluctuated between 45,000 and 99,000 tonnes per year during the last decades of the 20th century, with the highest dust emissions recorded in 1991 (Ots and Mandre, 2012). In addition to emissions from the cement factory, the site has also received emissions from nearby industries and oil shale power plants, including the Balti power plant, located approximately 100 km west, and the Aru-Lõuna limestone quarry, situated 8 km to the east (Karofeld, 1996, Figure 1) which supplies raw materials for cement production at Kunda. However, significant emission reductions occurred

https://doi.org/10.5194/egusphere-2025-1351
Preprint. Discussion started: 17 April 2025

after 1996, following the installation of pollution control filters, which lowered emissions from 14,000 tonnes in 1996 to 530 tonnes in 2000 and 8 tonnes in 2020 (Figure 3).

The input of alkaline cement dust emissions has generated the drastic pH increase of bog's water. During 1996-1997, the pH levels taken from peat pools at Varudi varied from 7.6 to 8.5, whereas in natural conditions bog pools have a pH in the range of 3-4. Disturbances at the site are compounded by drainage and peat harvesting for horticulture, which continues to the present day, with harvesting affecting around 40% of the former centre of the site (Figure 1C).

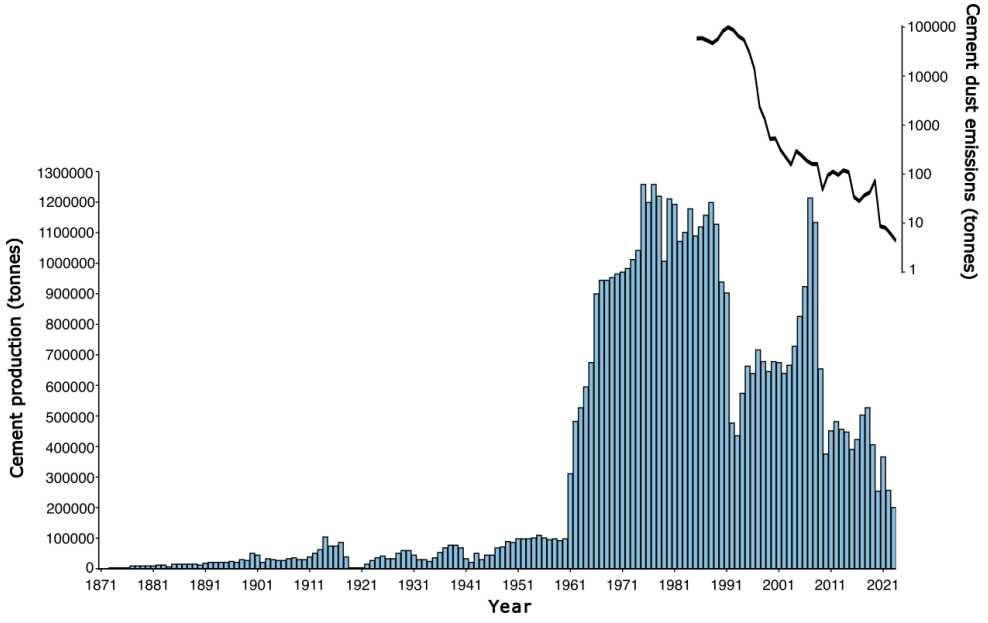

Figure 3. Cement annual production and emissions by the Cement Factory in Kunda. Data adapted from Trumm *et al*., (2010), digitised from a figure at page 209 using WebPlotDigitiser: https://automeris.io/WebPlotDigitizer/ Emissions data (available from 1985 to 2023) sourced from Raukas (1993); Pärtma (2023) and Heidelberg Materials Kunda AS (2023). Note the logarithmic scale for emission values.

The chemical composition of the cement dust emissions from Kunda consists primarily of CaO (12 – 17%), SiO_2 (6 – 9%), and several other trace metals, including lead (Pb, c. 60 mg kg^{-1}), cadmium (Cd, c. 0.9 mg kg^{-1}), and zinc (Zn, 129 mg kg^{-1}) (Mandre and Ots, 1999). The pH of the cement dust in the water solution ranged between pH 12.3 to 12.6 (Mandre and Korsjukov, 2007).

2.2. Coring method

In August 2022, an 86 cm peat core (VAR1) was extracted from Varudi peatland using a 1-meter-long Wardenaar peat corer (Wardenaar, 1987, coring location: 59°26'23"N,

https://doi.org/10.5194/egusphere-2025-1351
Preprint. Discussion started: 17 April 2025

26°35'55"E, Figure 1D). The core site was located near an actively harvested peat area but is within an intact section of the site in what was originally the bog's central raised dome. Vegetation was characterised by *Pinus sylvestris*, with the ground cover dominated by *Eriophorum* spp., *Menyanthes trifoliata*, *Vaccinium* spp., and scattered *Betula nana*. Both *Sphagnum* and brown mosses were also present. Despite its proximity to a drainage ditch, the coring location was representative of the overall condition of the site.

Following recovery, the core was wrapped in plastic and transported to the Faculty of Geographical and Geological Sciences at Adam Mickiewicz University, Poznań, Poland for analysis. The core was stored at 4 °C prior to sub-sampling.

2.2. Dating methods and age-depth model

Identifiable above-ground plant macrofossils were picked from 1 cm thick sub-samples taken at various depths throughout the core, following frameworks by Piotrowska *et al*. (2011) and Nilsson et al. (2001). *Sphagnum* stems, branches and leaves were preferentially used for dating where present. Where these were not available, above-ground remains of ericaceous plants (leaves, stems, seeds) were used instead. Initial samples were taken at 20 cm intervals throughout the core to establish a baseline chronology, which was then used to determine where additional samples would be selected. A total of 12 samples were sent for radiocarbon analysis. Each sample was pre-treated using the acid-base-acid approach and analysed by accelerator mass spectrometry (AMS) at the Poznań Radiocarbon Laboratory, Poland.

To provide a reliable chronology for recently accumulated peat, ^{210}Pb and $^{239+240}$Pu analyses were used on material from the upper 40 cm of the core at 1 cm contiguous resolution, following methods outlined by Appleby (1998). Peaks in the activity of $^{239+240}$Pu, which are linked to nuclear fallout events (e.g., 1950s atmospheric nuclear tests), were also measured as independent time-markers to validate and supplement the age-depth model (Mroz *et al.,* 2017; Cwanek *et al.,* 2021). Samples were processed at the Polish Academy of Sciences' Institute of Nuclear Physics, Kraków, Poland using an AlphaAnalyst™ 7200 spectrometer (Mirion Technologies). Quality control and accuracy was ensured by measuring blanks and certified reference material (IAEA 447, IAEA 385) alongside the core samples (results are provided in Supplementary Table 1. The activity concentration of ^{210}Pb (T 1/2 =22.3 yr) was estimated by measurement of its decay product - ^{210}Po (T 1/2 = 138.4 d), while $^{239+240}$Pu was

https://doi.org/10.5194/egusphere-2025-1351
Preprint. Discussion started: 17 April 2025

measured directly. Activity concentrations of ^{210}Pb and $^{239+240}$Pu are reported in units of Bq kg^{-1}.

The age-depth model was constructed by integrating all ^{14}C, ^{210}Pb, and $^{239+240}$Pu data within a Bayesian framework in R using the package 'rplum' (rplum package, Aquino-López *et al.,* 2018; Blaauw *et al.,* 2021; R working group, 2023). rplum generates maximum age probabilities at user-defined intervals (here every 1 cm), together with maximum and minimum ages based upon calculated 95% credible intervals. This method allows for the integration of ^{14}C dates with the ^{210}Pb dates without the need for re-modelling (Aquino-López *et al.,* 2018, 2020). Radiocarbon dates were calibrated in rplum using the INTCAL20 curve, with post-1950 samples using the BOMB1 curve for the Northern Hemisphere (Reimer *et al.,* 2020; Uno *et al.,* 2013). In this study, the resultant ages are expressed as calendar years (cal) CE, with 0 BP equal to 1950 cal CE.

2.3. Palaeoenvironmental proxies

2.3.1. Testate Amoebae

Samples were processed following a modified version of protocols by Hendon and Charman (1997). Samples were placed into 50 ml centrifuge tubes filled with deionised water and agitated for c. 10 minutes. These were sieved through a 300 µm mesh and the smaller fraction was retained. Sieved samples were centrifuged at >3000 rpm for 5 minutes and a sub-sample of the resultant material was transferred to a microscope slide for identification at 400x magnification. Samples were not heated or micro-sieved, to retain small but ecologically sensitive species, as recommended by Avel and Pensa (2013). A minimum count of 100 tests for each sample was considered statistically significant (Payne and Mitchell, 2008). Tests were identified to the species level where possible, with reference to Siemensma (2023) and Mazei and Tsyganov (2006), and were later pooled into taxonomic groups defined by Amesbury *et al.* (2016). The relative abundance (%) of each taxa count was calculated for each sample. Water table depth and peat pore water pH were reconstructed using the pan-European tolerance down weighted with inverse de-shrinking transfer function model by Amesbury *et al.* (2016), based on a training set of 1302 samples spanning 35° of latitude and 55° of longitude. Reconstructions were performed using the 'Rioja' package in R (Juggins, 2019). Small species (<10-25 µm, broadly oval-shaped) not included in these groupings but present in the core from Varudi were grouped under the '*Cryptodifflugia oviformis*' group.

https://doi.org/10.5194/egusphere-2025-1351
Preprint. Discussion started: 17 April 2025

Stratigraphically Constrained Cluster Analysis (CONISS) was used to quantitatively define stratigraphic zones in the sub-fossil testate amoeba data (Grimm, 1987). This method is used to determine statistically significant zones, reflecting changes in testate amoebae community composition. the data were square root transformed prior to applying CONISS. The numbers of statistically significant zones were determined using Broken-Stick modelling.

We applied the framework outlined by Burge *et al.* (2023) to identify significant ecological transitions in the testate amoeba communities due to disturbance. Sub-fossil data were Hellinger transformed and analysed using the 'prcurve' function in the 'analogue' package in R (Simpson and Oksanen, 2016). Principal response curves, which reduce multi-dimensional community data to a single-dimensional curve, calculating the (dis)similarity between sample scores indicative of the difference between samples (De'ath, 1999; van Den Brink and Braak, 1999) provided the best fit for our data. A generalised additive model (GAM), an approach effective in capturing rapid and non-linear changes in palaeoecological studies, was applied to the PrC data to account for temporal autocorrelation (Auber *et al.,* 2017; Beck *et al.,* 2018; Burge *et al.,* 2023). Given the abrupt changes in our data, we also applied an adaptive spline GAM following Burge *et al.* (2023). However, this method does not account for temporal autocorrelation and thus remains incompatible with the GAM framework as outlined by Simpson (2018).

2.3.2. Plant macrofossils

Plant macrofossil analysis followed procedures adapted from Mauquoy *et al.* (2010). Samples of approximately 5 cm^3 were sieved through a 200 μm test sieve and the larger fraction was retained. Botanical composition was estimated as percentages under a low-powered microscope at a 10–100× magnification, using a 10 x 10 eyepiece graticule for quantification. Seeds, fruits, spindles, leaves, and wood were also identified at the species level where possible and counted as individual counts. Identification was aided by identification guides (Katz *et al.,* 1965, 1977; Grosse-Brauckmann, 1972, 1974; Tobolski, 2000; Mauquoy and van Geel, 2007; Bojnanský and Fargašová, 2007). *Sphagnum* remains were identified to sub-generic sections, with 100 leaves examined per sample, where possible, to calculate the relative abundance of each sub-section as a percentage of the total leaves identified.

https://doi.org/10.5194/egusphere-2025-1351
Preprint. Discussion started: 17 April 2025

2.3.3. Pollen, non-pollen palynomorphs and microscopic charcoal analyses

Past changes in vegetation cover at the landscape scale were assessed using pollen analysis (Seppä and Bennett, 2003). A total of 22 samples were prepared following the laboratory procedures outlined by Berglund and Ralska-Jasiewiczowa (1986). Each 1 cm thick sample, measuring 1 cm^3, was sub-sampled at 5 cm intervals throughout the core. The samples were treated with 10% potassium hydroxide (KOH) to remove humic compounds before acetolysis. A *Lycopodium* tablet (batch no: 280521291, 18,407 spores per tablet; Manufacturer: Lund University) was added to each sample to calculate pollen concentrations, following methods by Stockmarr (1971). Samples were transferred to microscope slides and mounted in glycerine jelly for analysis. Pollen, spores, and selected non-pollen palynomorphs (NPPs) were identified and counted using a high-powered stereo microscope. Identification was based on established atlases and keys (Pollen: Moore *et al.,* 1991; Beug, 2009; NPPs: van Geel, 1978; van Geel and Aptroot, 2006; Miola, 2012). Although a target of 500 terrestrial pollen grains was aimed for per sample, this count was not always achievable due to low pollen concentrations in some core sections. The relative abundance of spores and NPPs was calculated as a proportion of the terrestrial pollen sum (TPS), which includes both arboreal (AP) and non-arboreal (NAP) pollen, excluding aquatic and wetland plant spores, Ericaceous pollen, and NPPs.

In addition to pollen counts, microscopic charcoal particles (> 10 - < 100 µm) were counted from pollen slides as past fire activity, both natural and anthropogenic (Finsinger and Tinner, 2005), while spheroidal carbonaceous particles (SCPs) counted as indicators of industrial activity (Patterson III *et al.,* 1987; Swindles, 2010). Microcharcoal concentrations per cm^3 were calculated by dividing the number of particles counted with the number of *Lycopodium* spores and multiplying this by the total number of particles counted, and accumulation rates (reported as particles cm^{-3} yr^{-1} were calculated by dividing the pollen concentration with the rPlum-derived age increments per cm slice.

2.3.4. Apparent rates of carbon accumulation

To measure apparent rates of carbon accumulation (aCAR), contiguous 1 cm-thick sub-samples were taken throughout VAR1. The volume of each wet sample was determined by water displacement, and then the samples were dried in an oven at 105 °C until no further

https://doi.org/10.5194/egusphere-2025-1351
Preprint. Discussion started: 17 April 2025

weight loss occurred. Dry bulk density was calculated by dividing the wet volume by the dry mass of each sample. Organic matter content (derived from LOI) was determined by ashing the samples at 550 °C for six hours, following the method of Chambers *et al.* (2011).

The carbon content of each sample was estimated indirectly by multiplying the LOI content by 0.52, based on the average ratio of organic carbon (OC) and LOI in ombrotrophic peat from multiple studies (Ball, 1964; Dean, 1974; Gorham, 1991; Clymo *et al.,* 1998). Carbon density was calculated by multiplying the dry bulk density (g cm^3) by the percentage of carbon content, as described by Chambers *et al.* (2011). Apparent carbon accumulation rates (aCAR) were then calculated by dividing the carbon density from each peat slice by the sedimentation rate, determined from the age-depth model (Young *et al.,* 2019, 2021).

2.3.5. µXRF-Core Scanning (ITRAX)

To identify the section of the core affected by cement dust pollution, we followed methods similar to those used by Varvas and Punning (1993) to assess pollution histories from Estonian lake sediments. They identified rapid increases in micro-element concentrations associated with alkaline fly-ash emissions, accompanied by a decrease in organic matter, indicating the presence of particulate emissions from oil-shale combustion by power plants.

In this study, the concentrations of geochemical elements throughout the core were measured using an ITRAX µXRF core scanner equipped with a molybdenum X-ray tube. Element concentrations were quantified as counts per second, based on the number of secondary fluorescence detected for each element over a given period. Measurements were taken at 5 mm intervals (30 kV, 50 mA, exposure time: 30 seconds per step) at the Institute of Geography, University of Bremen, Germany. The scanner identified the activity of the following elements: Al, Si, P, S, Ar, K, Ca, Sc, Ti, V, Cr, Mn, Fe, Co, Ni, Cu, Zn, Ga, Ge, Se, Br, Rb, Sr, Y, Ba, Pt, Pb, Bi, and Fe.

The mean concentrations of each element were calculated for each 1 cm slice of the core. To account for variability in element concentrations due to sedimentation throughout the core, the results were normalised by dividing the total counts by the sum of the coherent and incoherent peaks, following the approach of Orme *et al.* (2015) as recommended by Longman *et al.* (2019). The chemical signature of cement dust was identified based on the composition

https://doi.org/10.5194/egusphere-2025-1351
Preprint. Discussion started: 17 April 2025

of clinker emissions from the Kunda Cement factory, as detailed by Klõšeiko *et al.* (2011). Due to the uneven and unconsolidated nature of the top 6 cm of the core, this section was not scanned and was removed prior to analysis.

Principal Component Analysis (PCA) was used to summarise patterns of variation in the geochemical data, using the 'vegan' package in R (Oksanen *et al.,* 2019). To mitigate scaling effects, the data were standardised to z-scores. The analysis was conducted with varimax rotation in correlation mode, to explore correlations between elements and organic matter percentage (Silva-Sanchez *et al.,* 2014). The number of components to retain for analysis was determined using a Broken-Stick model.

3. Results.

3.1. Dating and age-depth model.

A total of 13 radiocarbon dates were analysed from core VAR1, four of which were post-bomb dates extending to a depth of 19.5 cm. The oldest dated section of the core produced a date of > 1000 yr. Radiocarbon and calibrated dates are shown in Table 1.

Table 1. Uncalibrated and calibrated radiocarbon dates from core VAR1, including depths and materials used for dating. PMC = Percent modern carbon

Code	Depth (cm)	Radiocarbon Age + error	Material dated	Calibrated dates + uncertainties
Poz-164520	5.5	104.51 ± 0.33 pMC	Seeds, ericaceous leaves	68.3% probability 1950 – 1957 (5.6%) 2010 – 2012 (62.7%) 95.4% probability 1956 – 1957 (10.6%) 2009 – 2012 (79.9%) 2012 – 2013 (5%)
Poz-164521	9.5	110.06 ± 0.67 pMC	Seeds, ericaceous leaves	68.3% probability 1957 – 1958 (7.5 %) 1997 – 1999 (50%) 1999 – 2000 (10.8%) 95.4% probability 1958 (11.2 %) 1996 – 2001 (85.2 %)
Poz-164662	15.5	110.36 ± 0.48 pMC	Seeds, ericaceous leaves	68.3% probability 1958 (7.3%) 1997 – 1999 (56.9%) 2000 (4.1%)

https://doi.org/10.5194/egusphere-2025-1351
Preprint. Discussion started: 17 April 2025

				95.4% probability 1958 (11.9%) 1997 – 2000 (80.3%)
Poz-161987	19.5	118.8 ± 0.67 pMC	*Sphagnum* stems, leaves, branches	68.3% probability 1986 (68.3%) 95.4% probability 1959 (5.4%) 1960 (3.4%) 1986 - 1989 (86.7%)
Poz-162663	26.5	80±30	*Sphagnum* stems, leaves, branches	68.3% probability 1697 - 1724 (22.0%) 1814 - 1837 (20.1%) 1881 - 1913 (26.1%) 95.4% probability 1691 - 1729 (26.2%) 1809 - 1922 (69.3%)
Poz-164664	34.5	80±35	*Sphagnum* stems, leaves, branches	68.3% probability 1695 - 1725 (21.6%) 1813 - 1839 (19.6%) 1878 – 1916 (27.1%) 95.4% probability 1686 - 1725 (26.4%) 1805 - 1929 (69.0%)
Poz-161988	39.5	105±30	*Sphagnum* stems, leaves, branches	68.3% probability 1695 - 1725 (19.9%) 1813 - 1839 (17.5%) 1846 – 1853 (4%) 1869 - 1872 (1.4%) 1878 - 1916 (25.5%) 95.4% probability 1683 - 1737 (25.9%) 1803 - 1937 (69.5%)
Poz-163962	49.5	540±30	*Sphagnum* stems, leaves, branches	68.3% probability 1329 – 1338 (8.5%) 1397 - 1428 (59.8%) 95.4 % probability 1323 - 1357 (26%) 1392 - 1437 (69.5%)
Poz-161989	59.5	865±30	*Sphagnum* stems, leaves, branches	95.4% probability 1153 - 1263 (87.2%)
Poz-163963	69.5	875±30	*Sphagnum* stems, leaves, branches	95.4% probability 1126 - 1231 (79.2%) 1243 - 1258 (1.8%)
Poz-161990	79.5	910±30	*Sphagnum* stems, leaves, branches	68.3% probability 1047 - 1085 (28.6%) 1097 - 1103 (2.8%) 1126 - 1179 (30%) 1192 - 1205 (1.8%) 95.4% probability 1041 – 1214 (95.4%)

https://doi.org/10.5194/egusphere-2025-1351
Preprint. Discussion started: 17 April 2025

Poz-161992	85.5	985±30	*Sphagnum* stems, leaves, branches	68.3% probability 1022 - 1048 (26.8%) 1084 - 1128 (34.7%) 1140 - 1150 (6.8%) 95.4% probability 994 – 1055 (38.7%) 1076 – 1158 (56.7%)

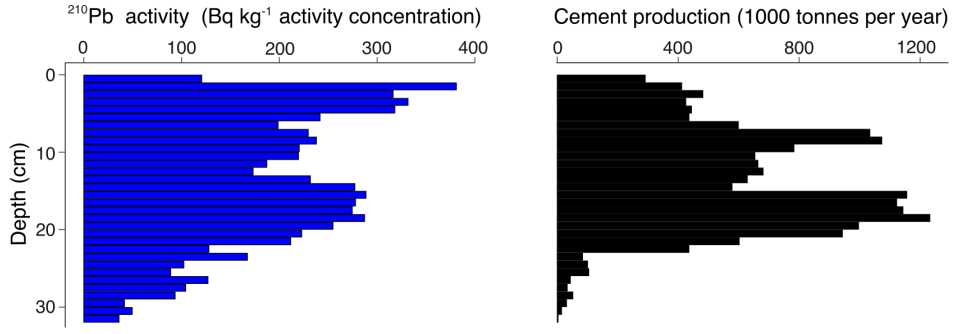

Figure 4. Comparison between ^{210}Pb activity concentrations throughout core VAR1 and cement production. Values interpolated from a GAM fitted to annual cement production data from Kunda Cement Factory (Figure 2; Trumm *et al.*, (2010)) at the same age frequency as the VAR1 age depth model, Figure 5) using a GAMM.

The ^{210}Pb activity profile throughout core VAR1 (Figure 4) declined throughout the core, although not in a typical monotonic pattern, with a substantial increase from 12.5 cm to 19.5 cm, indicating that the rate of ^{210}Pb accumulation was not constant throughout the core. This spike is due to the enrichment of ^{210}Pb from fly-ash fallout from the cement factory and other sources (Vaasma *et al.,* 2014; 2017). Comparison of the ^{210}Pb activities and cement production rates applied to the age-depth model until 1996 support this (Figure 4) with a significant correlation (τ_b = .487, p = <.0001), indicating that ^{210}Pb accumulation in the core cannot be solely attributed to precipitation. From 32 cm core depth, ^{210}Pb activities achieve low levels, although they do not reach the background activity. Unsupported ^{210}Pb was calculated using linear regression of the last 5 samples, showing that the samples assumed background activities following the final measured samples.

The $^{239+240}$Pu activity profile reflects the history of atmospheric deposition at the site (Figure 5). A clear peak at 28.5 cm corresponds to the onset of nuclear testing in 1945, followed by a second, larger peak at 22.5 cm, likely associated with the peak in global fallout from bomb testing in 1963, before the signing of the Partial Test Ban Treaty (Cwanek *et al.,* 2021). Smaller

https://doi.org/10.5194/egusphere-2025-1351
Preprint. Discussion started: 17 April 2025

peaks at 16.5 cm suggest possibly the 1986 Chernobyl fallout (Ketterer *et al*., 2004), and at 5.5 cm potentially originate from the 2011 Fukushima disaster (Bossew, 2013).

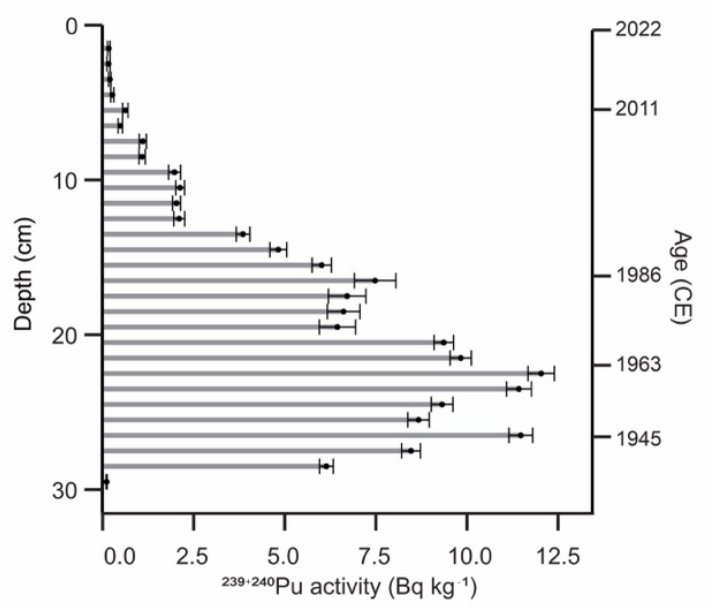

Figure 5. $^{239+240}$Pu activity with depth in core VAR1. Selected median dates from the rPlum-derived age-depth model show good correspondence between known fallout events. Each peak may be tentatively related to a known nuclear fallout event, as shown on the right y-axis.

The age-depth relationship for core VAR1 (Figure 6) was calculated by aligning ^{210}Pb and $^{239+240}$Pu data with the calibrated radiocarbon dates. Considering the enrichment of ^{210}Pb from industrial fallout, the assumption of a constant unsupported ^{210}Pb supply was violated. Despite this, anchoring the model with the known 1963 peak in $^{239+240}$Pu activity and adding a constant but uncertain reservoir effect of c. 15 years for radiocarbon dates improved the model alignment with the peaks in $^{239+240}$Pu. A radiocarbon reservoir effect is possible in *Sphagnum* peatlands, due to the recycling of 'old' gaseous carbon by mycorrhizal fungi associated with ericaceous plants near the peat surface. However, this does not usually occur when individual plant remains are dated, as was the case for our study (Piotrowska *et al.,* 2011).

The resulting age-depth model (Figure 6) indicates that peat accumulation rates were stable from the base of the core until around 1255 cal CE, after which accumulation slowed to around 0.22 yr cm^{-1}, remaining low until around 1940 cal CE, where there was a sharp acceleration to c. 2 yr cm^{-1}

https://doi.org/10.5194/egusphere-2025-1351
Preprint. Discussion started: 17 April 2025

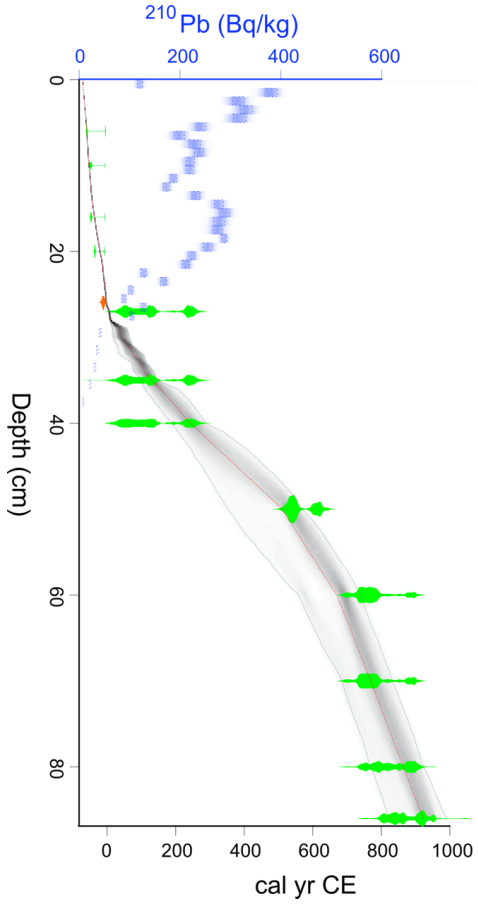

Figure 6. Age-depth model for core VAR1, including calibrated radiocarbon dates and uncertainty (green) ^{210}Pb activity (Bq kg^{-1}) in blue and the calendar date for the 1963 nuclear treaty peak (orange). Uncertainties for the model are shown as the shaded area.

3.2. Peat physical and chemical properties

Figure 7 shows that activities of elements associated with clinker dust pollution began to increase around c. 1873 cal CE, marking the beginning of cement production in Kunda. There is evidence of increasing lithogenic dust deposition throughout the core, beginning as early as the mid-12th century. There is a clear negative correlation between the activities of lithogenic elements associated with cement dust (Ti, Pb, Ca, K, Fe, Cr) and organic matter content, most noticeably between c. 1942 - 2006 cal CE, where lithogenic element activities increase. Organic matter content falls sharply until c. 1988 cal CE, suggesting the accumulation of cement dust occurred during this period, mirroring the results of studies in

https://doi.org/10.5194/egusphere-2025-1351
Preprint. Discussion started: 17 April 2025

NE Estonia lakes impacted by oil shale powerplants (Varvas and Punning, 1993; Punning *et al.,* 1996; Koff *et al.,* 2016).

The aCAR for the Varudi core is illustrated in Figure 7, which also shows the trends in LOI %, bulk density, and carbon accumulation throughout the core. Over the past millennium, the average aCAR for the entire core is 148.7 g OC m^2 yr^{-1}. This is especially high in the upper section of the core, where carbon accumulation rates peak at 342.2 ± 231.7 g OC m^2 yr^{-1}. For most of the record (c. 1045 to 1910 cal CE), the mean aCAR is 72.9 ± 28.9 g OC m^2 yr^{-1}, aligning more closely with average values reported for Northern peatlands (Roulet *et al.,* 2007). The rate of carbon accumulation is relatively stable from the base of the core until c. 1280 cal CE, with aCAR averaging 94.5 ± 19.8 g OC m^2 yr^{-1}. After this point, aCAR falls to 51.3 ± 19.7 g OC m^2 yr^{-1}, remaining low until c. 1840 cal CE. After this date, aCAR increases significantly, reaching an average of 256.6 ± 221.2 g OC m^2 yr^{-1}.

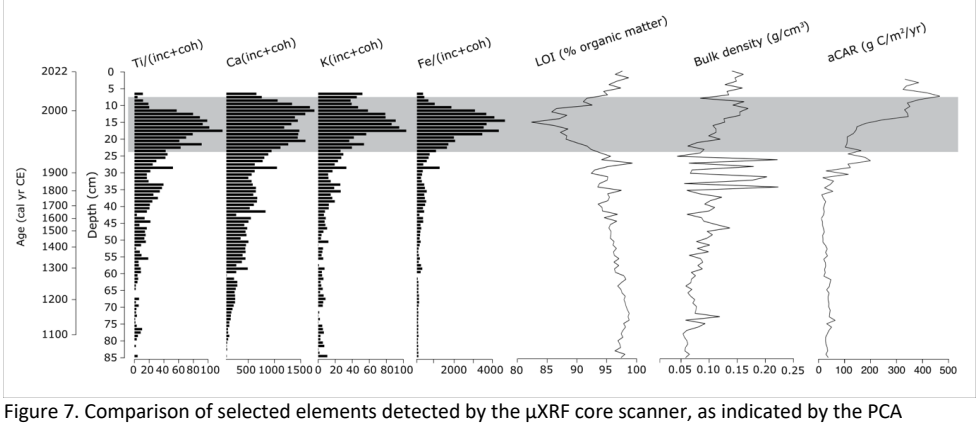

Figure 7. Comparison of selected elements detected by the µXRF core scanner, as indicated by the PCA analysis, for the detection of dust fallout from the Kunda Cement Factory. In addition to peat physical property parameters: Loss on ignition (LOI%), bulk density and apparent carbon accumulation rates (aCAR). µXRF Data are presented as counts per second and normalised by dividing the sum of incoherent (inc) and coherent (coh) activities. The shaded area represents the section of core where most of the cement dust is concentrated. The uppermost aCAR sample was removed from the figure to aid interpretation.

The broken stick model showed that the two first components together a significant proportion (48.3%) of the total variance in the peat's chemical composition (PCA1: 25.5%, PCA2: 22.8%). These components highlighted elements associated with clinker dust deposition from the Kunda Cement Factory and are significantly negatively correlated with peat LOI content (Figure 8).

https://doi.org/10.5194/egusphere-2025-1351
Preprint. Discussion started: 17 April 2025

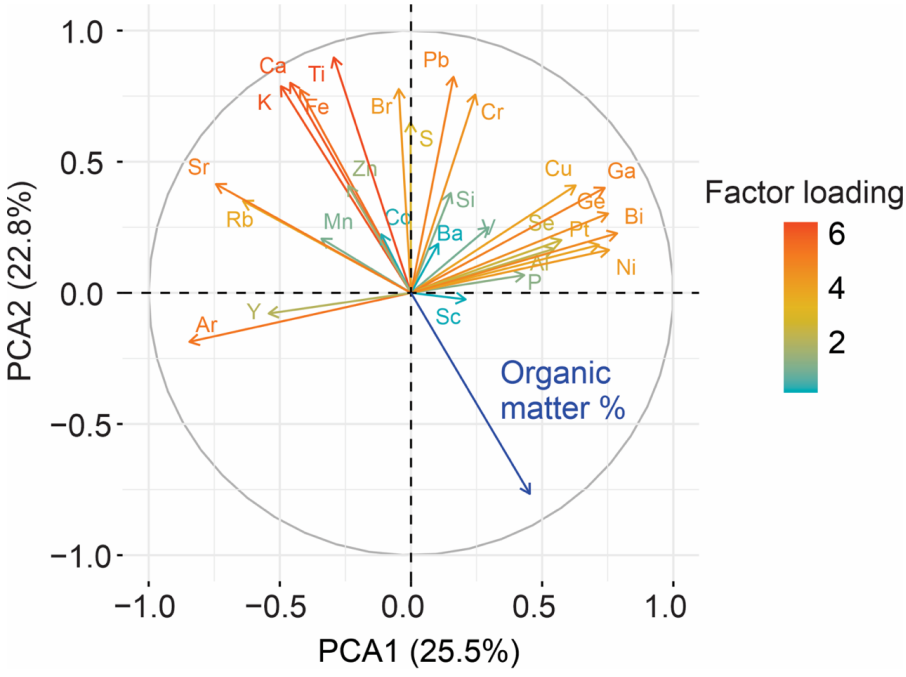

Figure 8. Biplot of first and second principal components showing factor loadings of individual elements scanned across core VAR1. Positively correlated variables point to the same side of the plot, while negatively correlated elements point to the opposite sides. Peat organic matter % (Derived from Loss on Ignition) content is shown in blue. The colour of the lines represents the sum factor loading of each variable for both axes, representing how strongly each variable contributes to the principal component.

3.3. Palaeoecological reconstructions

3.3.1. Plant Macrofossils

The results of plant macrofossil analysis are illustrated in Figure 9. The plant macrofossil data show three major phases of vegetation change, corresponding broadly with shifts observed in the testate amoeba and palynological records (Figures 10, 11 and 12).

https://doi.org/10.5194/egusphere-2025-1351
Preprint. Discussion started: 17 April 2025

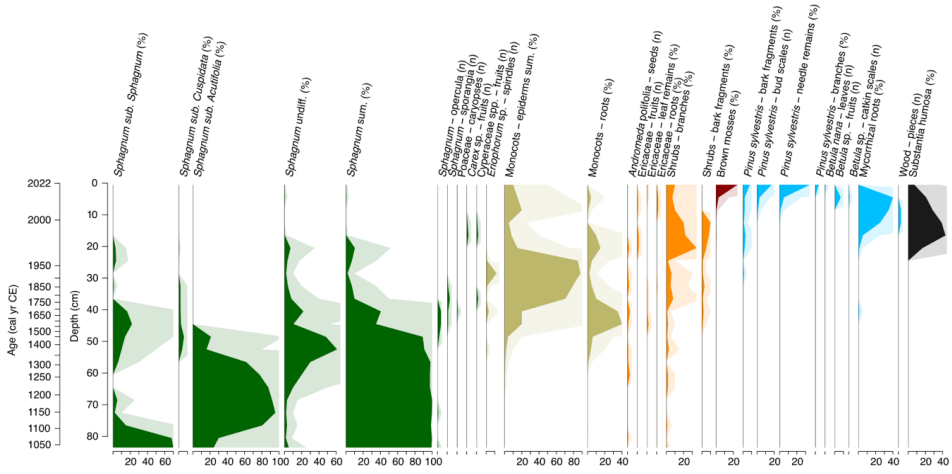

Figure 9. Plant macrofossil stratigraphic diagram illustrating the changes in the botanical composition throughout core VAR1. Note the mixed data types used, percentages and total counts.

From c. 1000 cal CE, the site is dominated by *Sphagnum* mosses, particularly those of the subgenus *Sphagnum*, although by the beginning of the 12th century, *Sphagnum sub. Acutifolia* becomes the most abundant. By c. 1450 cal CE, there was an increasing abundance of monocots, likely from *Eriophorum* species and Cyperaceae, owing to the presence of spindles and fruits identified to these species. During this period, *Sphagnum* gradually declined, eventually disappearing entirely by the start of the next phase.

The latter portion of the record, starting c. 1970 cal CE, is characterised by a shift towards more 'woody' vegetation. Shrub-type taxa increase initially, followed by a rise in ligneous remains, particularly those of *Pinus sylvestris*. Mycorrhizal roots, bark fragments, and pine needles become significant components of the peat's botanical composition in the upper section. *Betula* is represented in the uppermost samples by its characteristic catkin scales and fruits, along with a *Betula nana* leaf recovered from the surface sample. This late phase is also characterised by a high percentage of unidentified organic material. At the top of the core, remains of the brown moss *Tomentypnum nitens*, characteristic of calcareous fens, were identified (Hájek *et al.*, 2021).

3.3.2. Testate amoeba sub-fossil communities

Throughout core VAR1, a total of 105 distinct testate amoeba taxa were identified. The results of the testate amoeba analysis and reconstructions are presented in Figure 10. Three distinct zones were identified throughout the record by CONISS.

https://doi.org/10.5194/egusphere-2025-1351
Preprint. Discussion started: 17 April 2025

The first zone, extending from the base of the core to 44.5 cm (c. 1600 cal CE) is characterised by a mix of proteinaceous and mixotrophic species, including *Archerella flavum* and *Hyalosphenia papilio*. Other abundant species in this zone include *Difflugia pulex*, *Phryganella acropodia*, *Assulina muscorum* and *Assulina seminulum*. The second zone, ending at 19.5 cm (c. 1980 cal CE), shows a replacement of the dominant species by *Galeripora discoides*, *Amphitrema stenostoma*, and xenosomic species such as *Cyclopyxis arcelloiodes*. By 35.5 cm (c. 1821 cal CE), mixotrophic species have almost disappeared, replaced by *Cyclopyxis euryostoma*, *Centropyxis aculeata*, *Difflugia ampullula*, *Difflugia brevicolla* and *Pseudodifflugia gracilis*. The final zone, at the top of the core, is dominated by *Centropyxis elongata*, *Centropyxis sylvatica*, *Plagiopyxis* spp., *Euglypha rotunda* type, and *Euglypha leavis*.

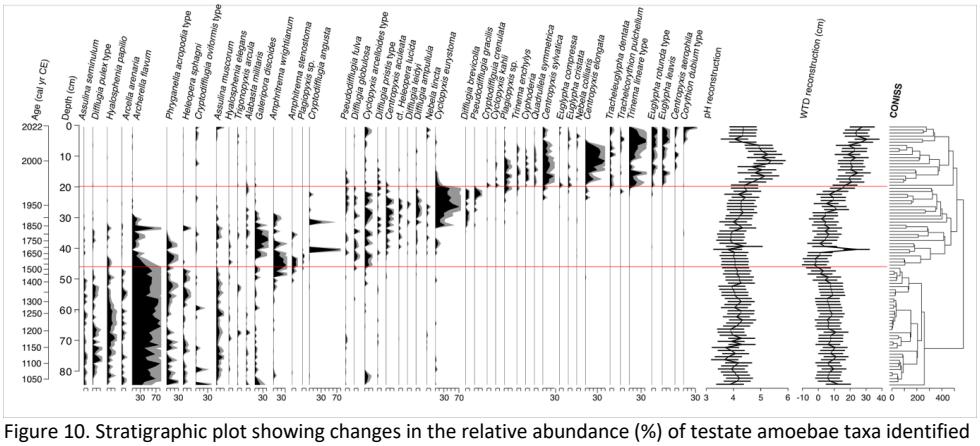

Figure 10. Stratigraphic plot showing changes in the relative abundance (%) of testate amoebae taxa identified throughout core VAR1, as well as reconstructed peat pore water pH and water table depths (WTD) and uncertainties. The results of CONISS are illustrated to the right of the figure, with horizontal red lines representing the zone boundaries defined by CONISS. Only species with maximum abundancies above 5% are illustrated. The full dataset is available in the supplementary data.

The relative abundance of testate amoeba taxa was used to reconstruct changes in water table depth and peat pore water pH over time. Both reconstructions exhibit notable trends throughout the past c. 1000 years. From the base of the core until c. 1330 cal CE, water table depths was relatively constant, averaging 7.0 ± 2.9 cm. Conditions became progressively wetter after this time, reaching a minimum of -2.5 cm by c. 1540 cal CE, possibly indicating a period of open water at the coring location. Water table depth began to decrease gradually, accelerating after c. 1960 cal CE and reaching a maximum by c. 2012 cal CE.

https://doi.org/10.5194/egusphere-2025-1351
Preprint. Discussion started: 17 April 2025

Reconstructed pH values were relatively stable throughout much of the record (4.1 ± 0.5). Around c. 1800 cal CE, pH began to rise, reaching a maximum of 5.4 ± 0.5 by c. 1998 cal CE. By c. 2006 cal CE until the top of the core, pH returned to pre-disturbance levels.

3.3.3. Pollen, spores, and non-pollen palynomorphs.

The results of the palynological analysis are illustrated in Figures 11 (Pollen and spores) and Figure 12 (Non-Pollen Palynomorphs- NPPs). The pollen sequence from the core VAR1 is dominated throughout by arboreal taxa, particularly *Pinus sylvestris* and *Betula* spp., with lesser contributions from shrubs such as *Calluna vulgaris* and *Vaccinium type*. The high dominance of these arboreal taxa and a low sampling resolution make detecting subtle shifts in human activity in the palynological record difficult to infer (Favre *et al.,* 2008). Other palynological studies from Estonia also report low variation in pollen assemblages and dominance of *P. sylvestris* and *Betula* across different regions, even during periods of significant land-use changes (e.g., Poska *et al*., 2004; Veski *et al.,* 2005; Łucówe *et al*., 2022).

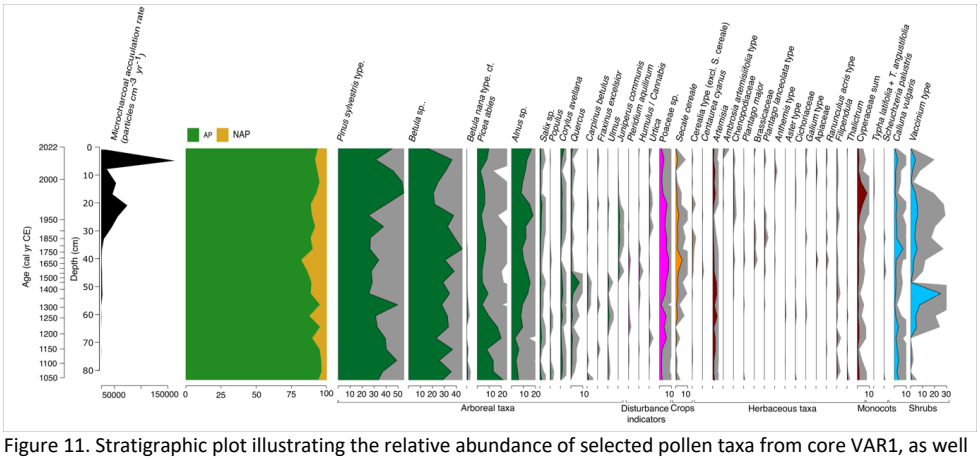

Figure 11. Stratigraphic plot illustrating the relative abundance of selected pollen taxa from core VAR1, as well as microcharcoal (expressed as the total number of counted fragments). Relative abundances of arboreal taxa are shaded green, disturbance indicators in pink, crops in orange, herbaceous taxa in brown and shrubs in teal. Grey shading represents 5x exaggeration. Only taxa with a minimum abundance of 2% are shown.

https://doi.org/10.5194/egusphere-2025-1351
Preprint. Discussion started: 17 April 2025

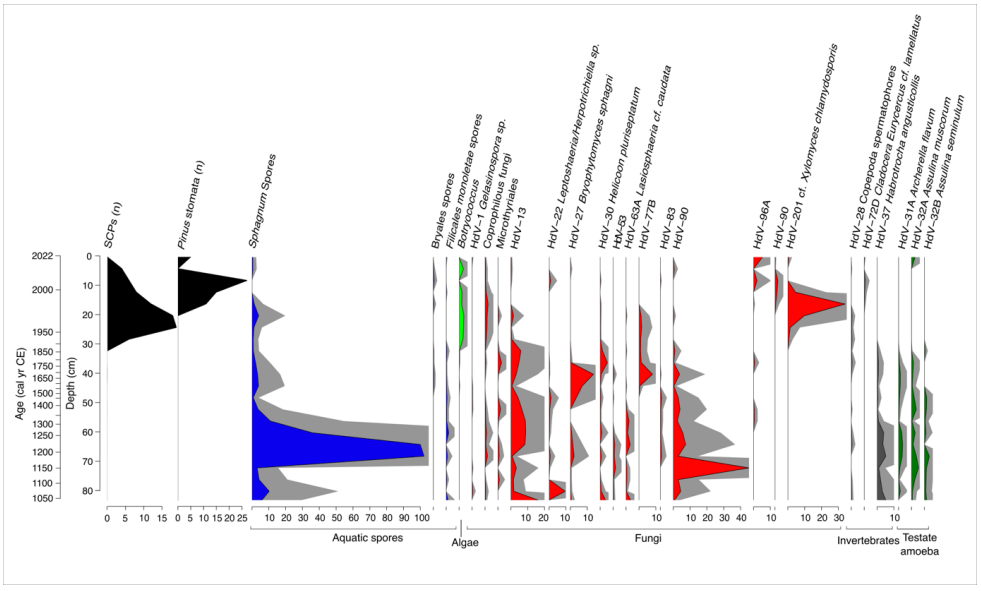

Figure 12. Stratigraphic plot illustrating the abundance of selected non-pollen palynomorphs from core VAR1, as well as spheroidal carbonaceous particles (SCPs) and *Pinus* stomata, both expressed as counts. Relative abundances of spores of aquatic taxa are shaded blue, algae: light green, fungi: red, invertebrate remains grey and testate amoebae in dark green. Grey shading represents 5x exaggeration. Only taxa with a minimum abundance of 2% are shown.

The oldest section of the core (c. 1000–1250 cal CE) provides little evidence of anthropogenic disturbance, indicating a largely forested landscape. This period is dominated by *Pinus sylvestris*, *Betula* spp., and *Picea abies*, suggesting a stable, predominantly woodland environment. After c. 1250 cal CE, there is a slight increase in pollen from grasses (Poaceae) from around 3% to c. 8% of the total assemblage until c. 1680 cal CE, as well as the appearance in low concentrations of plants indicative of disturbance, such as *Plantago lanceolata*, Chenopodiaceae and *Ranunculus acris* type and a general increase in *Secale* pollen which together may indicate low levels of agricultural activity, although wild populations of *Secale* are believed to have existed in Estonia (Veski, 1998; Poska et al., 2003). Despite this, arboreal pollen remains the dominant component of the record, with declines mainly affecting *Pinus sylvestris* (49 % at c. 1310 cal CE to 34% by c. 1680 cal CE) and *Picea abies* (16% at c. 1220 cal CE to 5% by c. 1680 cal CE). Tree species associated with early succession, such as *Betula*, remain largely unchanged, while *Alnus* increases during this period from c. 6% at the start of the record to c. 10% by c. 1680 cal CE. By c. 1680 cal CE, arboreal pollen has declined to its lowest relative abundance (around 82% of the total pollen sum). This decline is driven mainly by the changes in arboreal species, particularly declines in *P. sylvestris,* which becomes progressively less common through the core, a trend that continues until c. 1965 cal CE. By

https://doi.org/10.5194/egusphere-2025-1351
Preprint. Discussion started: 17 April 2025

c. 1680 cal CE a peak in cereals occurs, including *Hordeum*, although these are only present in low concentrations. The pollen record is stable after this period, with only slight (<1%) increases in *Calluna vulgaris* and *Vaccinium* type taxa occurring. These changes correspond with a rapid increase in microcharcoal accumulation rates, rising from 311 to 1027 particles cm^{-3} yr^{-1} following the opening of the cement factory, peaking at 9837 particles cm^{-3} yr^{-1} by c. 1970 cal CE. After this, *Pinus sylvestris* begins to recover, but the relative abundance of *Betula* spp. continues to rise. By c. 2010s cal CE, *Pinus sylvestris* becomes dominant once again, while *Betula* declines throughout the most recent samples, and microcharcoal accumulation reaches a maximum at c. 2010 cal CE, of 172237 particles cm^{-3} yr^{-1}.

The NPP record provides a more detailed picture of changes in the local environment than the pollen record. In the earliest portion of the record (c. 1000 - 1220 cal CE), fungi such as HdV-90 and HdV-13 (cf. *Entophlyctis lobata*) are common, and HdV-27 (*Bryophytomyces sphagni*) is present throughout. These fungi are typically associated with oligotrophic and ombrotrophic conditions, although HdV-90 can also thrive in more minerotrophic or poor-fen environments (van Geel, 1978; Kuhry, 1985).

Between c. 1220 - 1460 cal CE, HdV-13 increases in abundance. Around 1850 cal CE, taxa associated with the earlier section of the record start to decline, being replaced by the microalgae *Botryococcus* taxa, indicative of aquatic conditions in addition to several fungi including HdV-55A (*Sordaria* type), HdV-112 (*Cercophora* type). The most notable species in the upper section of the core during this period is HdV-201 (cf. *Xylomyces chlamydosporis*), a wood-inhabiting fungus linked to freshwater environments or pool vegetation (Goh *et al.,* 1997; Kuhry, 1997). This species is especially abundant c. 2006 cal CE, comprising around 34% of the assemblage. After c. 1950s cal CE, the diversity of NPPs declines. A key species identified in this section is *Botryococcus braunii*, a green alga typically found in environments with high levels of inorganic phosphorus, which peaks around 1985 cal CE (Órpez *et al.,* 2009) suggesting a shift toward more nutrient-enriched conditions. Overall, the record suggests a transition from nutrient-poor, *Sphagnum*-dominated peat towards an increasingly nutrient-enriched system, followed by a change towards decomposers of ligneous material.

3.3.4. Rate of change analysis

https://doi.org/10.5194/egusphere-2025-1351
Preprint. Discussion started: 17 April 2025

The principal response curves (PrC) explained 79% of the variance in the sub-fossil testate amoeba data from Varudi and are illustrated in Figure 13. The poor fit of GAM models to the PrCs prompted us to use adaptive splines with a GAM, which are recommended for data exhibiting abrupt changes (Burge *et al.,* 2023). However, adaptive spline GAMs cannot yet be used within the GAM framework as described by Simpson (2018). One outlier was removed due to the difference in testate amoebae composition owing to a high proportion of *Cryptodifflugia angusta* (33.5 cm).

The PrC revealed two separate periods of change at Varudi, as well as highlighting periods of rapid change associated with the onset of cement production in Kunda in 1871, and an earlier change indicated from the palynological record to coincide with increasing human activity in the landscape (Figure 11). Testate amoeba community composition was relatively consistent from c. 1040 cal CE until c. 1330 cal CE and again between c. 1645 to c. 1886 cal CE. Following c. 1998 cal CE, the direction of change in the PrC curve reverses, coinciding chronologically with the installation of filters in the cement factory in 1996. By the end of the record, testate amoeba community composition was characterised by the return of species such as *Cyclopyxis arcelloides*, *Cryptodifflugia oviformis*, and *Assulina muscorum*, which were not abundant since before c. 1970 cal CE.

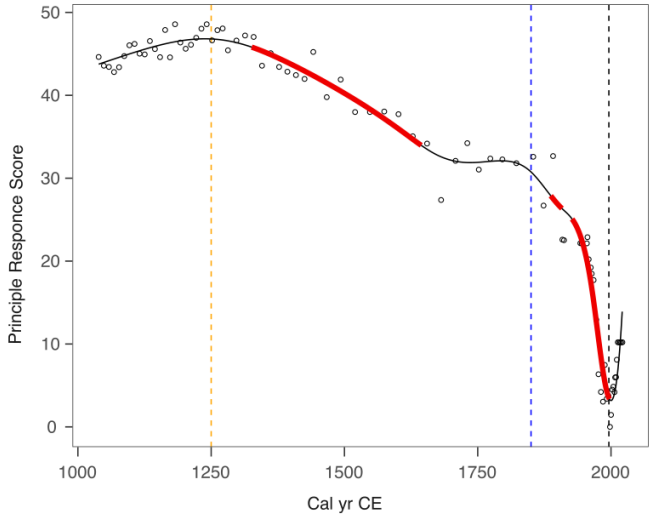

Figure 13. Changes in principle response curve scores derived from sub-fossil testate amoebae data, modelled using an adaptive spline generalised additive model GAM (black line). Solid red lines indicate periods of rapid change, identified where the modelled confidence interval of the slope does not include zero. Vertical dashed lines denote key chronological events potentially influencing environmental conditions at Varudi: The onset of human activity recorded in the pollen data (c. 1250 cal CE, orange), the beginning of cement production in Kunda (1871, blue) and the installation of pollution control filters at the cement factory (1996, black).

https://doi.org/10.5194/egusphere-2025-1351
Preprint. Discussion started: 17 April 2025

4. Discussion

4.1. Palaeoecological assessment of ecosystem and functional changes before, during, and after intensive alkaline dust pollution

The palaeoecological record of the Varudi peatland reveals three distinct phases of botanical change occurring over the past 1,000 years: an ombrotrophic bog phase (c. 1000–1250 cal CE), a poor fen phase (c. 1250–1570 cal CE), and a wetland forest phase that continues to the present day. Unlike most research on peatland recovery, which has typically been conducted on historically drained, mined, or agricultural sites (Roderfeld, 1993; Graf *et al.,* 2008; Wagner *et al.,* 2008; Paal *et al.,* 2010), our study presents a unique pre-disturbance context for understanding the effects of atmospheric pollution upon Estonian peatlands.

The different phases of development exhibited by the site in contrast with the different periods of anthropogenic activity and disturbance are summarised in Figure 14. During the early ombrotrophic phase, low palynological richness, minimal microcharcoal counts and abundant peat organic matter indicate a largely forested landscape with limited human impact near the site, consistent with other palaeoecological records throughout Estonia during this period (Veski *et al.,* 2005). The dominance of *Sphagnum* mosses and mixotrophic testate amoeba species such as *Archerella flavum* and *Hyalosphenia papilio* reflect the relatively undisturbed and productive nature of the bog during this phase (Marcisz *et* al., 2020; Łuców *et al.,* 2022). During this period, water table depths were high, and pH levels were low, consistent with natural conditions for ombrotrophic bogs in the Northern Hemisphere (Warner and Asada, 2006).

https://doi.org/10.5194/egusphere-2025-1351
Preprint. Discussion started: 17 April 2025

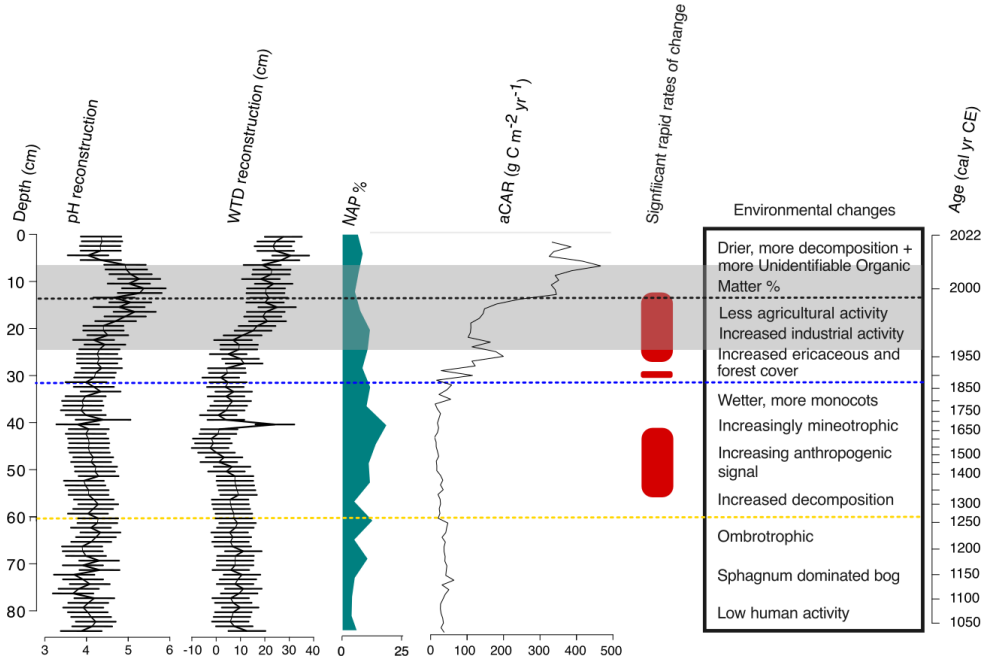

Figure 14: Summary of key trends in the Varudi peatland record. Shown are changes in reconstructed pH and water table depth, percentages of non-arboreal pollen (serving as a proxy for forest clearance related to agricultural activity), apparent carbon accumulation rates (aCAR), periods of significant change (as identified by principal response curves with Generalised Additive Models, GAMs), and a general timeline of environmental shifts. Dashed horizontal lines represent key historical events relevant to the Varudi record: the yellow line marks the approximate onset of human activity c. 1250 cal CE, possibly linked to the Livonian Crusades; the blue line indicates the establishment of the Kunda Cement Factory in 1871; the black line denotes the installation of effective filters at the Kunda Cement Factory; and the grey-shaded area highlights the section of the core with substantial cement dust, identified through LOI and µXRF core scanning.

The beginning of agricultural activity around c. 1250 cal CE is broadly coincident with the German-Danish crusaders occupation of Estonia starting in 1227 CE (Veski *et al.,* 2005). From c. 1250 to 1570 cal CE, increased Poaceae, *Secale cereale*, and field weed pollen indicates a shift toward more open, meadow-like conditions (Poska and Saarse, 2002; Niinemets and Saarse, 2009), which may relate to the environmental effects resulting from economic changes resulting from the Teutonic order crusades, similar to those identified by Brown and Pluskowski (2011) in a peatland record from northern Poland.

Declines in *Pinus sylvestris* and *Picea abies*, alongside increases in early successional species such as *Betula* and *Alnus*, and minute increases in microcharcoal accumulation rates (Figure 11) suggest land clearance using slash-and-burn methods in the surrounding landscape (Jaats *et al.,* 2010). While arboreal pollen remained dominant, indicating continued forest cover around the Varudi peatland, mineral soil enrichment of the peat suggests overland flow or

https://doi.org/10.5194/egusphere-2025-1351
Preprint. Discussion started: 17 April 2025

aeolian deposition resulting from land clearance. Similar patterns of early human-induced soil erosion have been recorded in peatland records from central Estonia (Heinsalu and Veski, 2010). This is reflected by decreasing organic matter content and increasing concentrations of lithogenic elements such as Ca and Ti, patterns like those observed in Estonian lake sediment records following land clearance events (Koff *et al.,* 2016; Vandel and Vaasma, 2018). Ti, a conservative lithogenic element, indicates soil erosion from the surrounding catchment (Boyle, 2001; Boës *et al.,* 2011). By c. 1570 cal CE, the site had transitioned into a wetter, more minerotrophic fen, indicated by the gradual replacement of *Sphagnum* by monocots such as *Carex* spp. and *Eriophorum vaginatum* in the plant macrofossil record (Figure 9). Nutrient enrichment due to soil erosion resulting from forest clearance and agricultural activities in the landscape at this time likely contributed to this shift (Hölzer and Hölzer, 1998).

The establishment of the Kunda cement factory in 1871 brought significant ecological changes to the site. Substantial increases in Ti, Ca, Fe, and other elements associated with cement dust fallout occurred along with increased pH and declining organic matter content, indicating the chemical influence of cement dust pollution upon the peat (Figures 7 and 8). This pollution appears to have driven rapid changes in testate amoeba communities by c. 1890 cal CE, as seen in the PrC record (Figures 13 and 14). These results are consistent with previous palaeoecological studies on alkaline pollution impacts in Estonian peatlands and lakes (Varvas and Punning, 1993; Koff *et al.,* 2016; Vandel and Vaasma, 2018; Vellak *et al.,* 2014). The enrichment of the peat by cement dust is reported to have had a fertiliser-like effect on ligneous and ericaceous species, increasing tree cover, size, and stand density within the industrial region of Estonia at this time (Pensa *et al.,* 2004; Ots *et al.,* 2011).

The concurrent hydrological changes experienced by the site, characterised by persistent water table lowering after c. 1960, were likely driven by drainage and enhanced transpiration rates following tree and shrub expansion onto the site (Stelling *et al.,* 2023). The simultaneous compounding effect of hydrological change upon the site confounds interpretation of the effects of alkaline pollution at Varudi peatland, as it is likely that the changes that occurred at this time were driven by the combined effects of both disturbances.

From 1955 CE onward, cement production increased, reflected in peaks of Ca, Ti, and K, alongside rising bromine (Br) levels, coincident with increased microcharcoal accumulation rates (increasing from c. 11 to 58 particles yr^{-1}. The halogen Br is often linked to changes in

https://doi.org/10.5194/egusphere-2025-1351
Preprint. Discussion started: 17 April 2025

storminess in peat palaeoecological studies due to being commonly sourced from marine aerosols (e.g., Shotyk, 1997; Turner *et al.,* 2014). Here, elevated Br levels correlate strongly with cement dust indicators, suggesting that increased Br in the core corresponds with enhanced plant decay and oxidation of abiotic organic matter, resulting in the formation of methyl bromide (Lee-Taylor and Holland, 2000; Keppler *et al.,* 2000). The increased presence of fungi in addition to microalgae species *Botryococcus braunii* in the palynological and plant macrofossil records further suggests that the soil decomposition rate increased during this period, coincident with periods of increased seasonal wetness (Barthelmes et al., 2012; Defrenne et al., 2023; Buttler et al., 2023; Thorman et al., 2003) (Figure 12).

Following the restoration of Estonia's independence in 1991, more rigorous environmental regulations resulted in a reduction of industrial emissions (Kask *et al.,* 2008). The effect of this decline is evident in our palaeoecological record, with declining pollution markers and pH returning to pre-disturbance levels after 1996 (Figures 7 and 10), as well as the apparent (albeit limited) recovery of testate amoeba communities shown by the PrC curve (Figure 13). Despite these improvements, the site has remained densely forested and enriched, with a persistently lowered water table. We find no evidence for botanical succession toward pre-disturbance conditions in the plant macrofossil record (Figure 9), while the presence of calciphilous *Tomentypnum nitens* at the core surface reflects the legacy of alkaline conditions (Malmer et al., 1992; Hájek et al., 2006; Apolinarska et al., 2024), likely resulting from the upward movement of mineral-rich water from deeper peat layers, although *Sphagnum* has returned to the site since its disappearance.

4.2. Ecosystem Recovery After Reduction in Atmospheric Alkaline Pollution

Our study found evidence of recovery in PrC of the sub-fossil testate amoeba assemblages (Figure 13). The community composition of these environmentally sensitive proxies showed signs of turnover nearly 30 years after installing filters at the Kunda cement factory. However, the extent of recovery indicated by the testate amoebae is limited, as the community composition in the top sediment layer more closely resembles conditions from c. 1977 cal CE, the peak period of cement production at Varudi (Figures 3 and 13).

We used adaptive spline GAMs to analyse our data, which while suitable for datasets exhibiting abrupt changes such as the example from Varudi (Burge *et al*., 2023), they cannot yet be incorporated into the Generalized Additive Mixed Model (GAMM) framework

https://doi.org/10.5194/egusphere-2025-1351
Preprint. Discussion started: 17 April 2025

described by Simpson *et al.* (2018) and are more susceptible to issues such as temporal autocorrelation and boundary effects (Simpson, 2018; Burge *et al.,* 2023). While the model best fit our data, more evidence is needed to draw conclusive interpretations about recovery than these results alone. More recently accumulated samples may be more influenced by temporal autocorrelation (Burge *et al.,* 2023). Some testate amoeba species may infiltrate the sub-fossil community composition downcore, making near-surface communities appear more similar (Liu *et al.,* 2024). Another limitation of this study is that our results are based upon reconstructions taken from a single core and as such do not account for the spatial heterogeneity characteristic of peatlands. Although palaeoecological trends tend to be well replicated across multiple cores within a given site (e.g., Barber et al., 1999; Hendon et al., 2001), it may be that the trends reconstructed from VAR1 represent conditions specific to the sampling site, rather than the whole site (Bacon et al., 2017). Paal *et al.* (2010) examined peatland vegetation communities in eleven bogs in northeastern Estonia at varying distances from sources of atmospheric alkaline pollution, finding evidence of *Sphagnum* re-establishment and the recovery of other bog-specific plant species at several sites as surface waters re-equilibrated to pre-pollution conditions, particularly within microforms that are less affected by contaminated groundwater. Therefore, recovery at Varudi may be spatially heterogenous, with some areas recovering more quickly depending upon their contact with polluted peat layers.

Studies investigating the recovery of vegetation communities following alkaline pollution show that ecosystem recovery may be limited due to the present, degraded condition of the ecosystem. For example, Vellak *et al.* (2014) studied bryophyte recovery following reductions in atmospheric fly-ash pollution across Estonia and northwestern Russian sites. They found that bryophyte species growing in more heavily affected sites tended to be adapted for growing in low light conditions, due to competing with the larger and more dense vascular plants that encroached on these sites, in response to the more enriched and alkaline conditions for which they are better adapted than bog-specific vegetation (Pärtel *et al.,* 2004; Zvereva *et al.,* 2008a, 2008b). Increased nutrient and litter supply and root exudates, coupled with the faster growth of vascular plants and trees may further hinder the reestablishment of bog and fen communities, delaying or preventing recovery (Konings *et al.,* 2019). Gunnarsson *et al.* (2002) demonstrated that nutrient enrichment, often accompanied by higher pH, can give vascular plants a competitive advantage over bog-specific vegetation (Limpens *et al.,* 2003; Dieleman *et al.,* 2015).

https://doi.org/10.5194/egusphere-2025-1351
Preprint. Discussion started: 17 April 2025

4.3. How has the pollution impacted apparent rates of carbon accumulation at the site?

Each of the phases in ecosystem development in the palaeoecological record corresponds with substantial changes in the apparent carbon accumulation rate (aCAR) throughout the Varudi record (Figure 7). Between c. 1000 to 1250 cal CE, when the site was in a relatively pristine, undisturbed condition, aCAR rates were higher (32.0 ± 10.7 g C m^2 yr^{-1}) than the average for northern hemisphere ombrotrophic peatlands (23 ± 2 g C m^2 yr^{-1}) (Korhola *et al.,* 1995; Yu *et al.,* 2009). Throughout the transition from bog to poor fen, from c. 1360 to 1570 cal CE, average aCAR rates increased initially (38.5 ± 34.3 g C m^2 yr^{-1}). However, they were highly variable, likely reflecting the incorporation of vascular plant roots from the overlying forested phase, introducing younger carbon into deeper sediments. Between c. 1630 and 1800 cal CE, rates fell as low as 19.0 ± 5.4 g C m^2 yr^{-1}, aligning with reported values for Finnish fens (Korhola *et al.,* 1995). Overall, minerotrophic fens typically exhibit lower carbon accumulation rates than ombrotrophic bogs (Loisel and Bunsen, 2020; Yang *et al.,* 2023).

Following the succession from poor fen to forested fen from c. 1871 cal CE to the present, there is an apparent increase in aCAR, especially in the most recently accumulated peat (280.7 ± 211.3 g C m^2 yr^{-1}). Due to the incomplete decomposition of labile organic matter at the peat surface, care must be taken when interpreting recently accumulated carbon from peat core records (Young *et al.,* 2019; 2021). This increase is likely due to high litter deposition from trees and shrubs, and the rapid decline in aCAR downcore suggests that this labile material is rapidly cycled back into the atmosphere rather than sequestered in the soil. Our results suggest that the current vegetation composition, dominated by trees and shrubs, is less effective for long-term carbon sequestration compared to earlier phases. While the water table remains reduced, the site shows limited potential for recovery to its original ombrotrophic condition due to ongoing drainage. At the same time, nutrient inputs and evapotranspiration from the overlying trees compound this limiting factor.

4.4. Indicators of critical thresholds to assess peatland condition and recovery due to alkaline pollution

By comparing our pH reconstruction with significant successional shifts at the site, we may infer the thresholds at which transitions in the steady state of the ecosystem occurred in response to changes in alkalinity at Varudi bog. Defining tipping points that may be broadly

https://doi.org/10.5194/egusphere-2025-1351
Preprint. Discussion started: 17 April 2025

applied to other sites allows for predicting ecosystem shifts in response to global change, allowing for prediction of such shifts in the future (Munson *et al.*, 2018). To our knowledge, our study is the first to define thresholds for tipping points in peatland ecosystems in response to changes in alkalinity.

Around c. 1800 cal CE, the reconstructed pH for Varudi showed an increasing trend from the previous, relatively stable conditions, reaching a maximum of 5.4 ± 0.5 by c. 1990s cal CE (Figure 10). This value aligns with pH measurements for polluted sites in Estonia, supporting the reliability of our reconstruction (Paal *et al.*, 2010). We find that the transition from an ombrotrophic bog to fen-like conditions, driven by mineral soil enrichment resulting from land clearance for agriculture in the surrounding landscape, was associated with an increase of pH levels from c. pH 3.8 to pH 4.1 which represents (due to the logarithmic scale of pH) nearly a twofold increase in alkalinity. Likewise, the subsequent shift from fen-like to forested conditions corresponded with a small average increase in pH to c. 4.3, or c. 1.5 times more alkaline than the previous state and more than three times more alkaline than during the bog phase. Our results suggest that relatively small increases in pH (increases in pH of 0.2 – 0.3) may result in critical ecosystem transitions. However, we stress that the threshold values defined here are highly uncertain, owing to the limited predictive ability of the transfer function models used for our pH reconstruction and the relatively significant uncertainties associated with transfer function models in general (Amesbury *et al.,* 2016). Higher pH values measured from bog pools at the site in 1996 – 1997 of 7.6 - 8.5 are higher than our estimates for this period, and by 2022 pH had only fallen to 6.3 - 6.8 (Pärtma, 2023), suggesting that our reconstruction underestimates pH levels experienced by the site by a wide margin. In addition, we cannot rule out the possibility that other impacts of cement deposition (e.g., reduced photosynthesis rates due to dust deposition) may have also played a role in driving botanical changes.

Contemporary field and lab experiments that manipulate the alkalinity of peatland soils directly may provide more precise values for ecosystem thresholds in response to alkaline pollution. However, to date few studies have done this for alkalinisation: one example is Kang *et al*. (2018) who conducted a series of field and laboratory pH manipulation experiments across seven peatlands in the UK, Japan, Indonesia and South Korea, finding that increases in pH resulted in significant changes in microbial composition, resulting in increased phenol

https://doi.org/10.5194/egusphere-2025-1351
Preprint. Discussion started: 17 April 2025

oxidase activity and enhanced DOC releases. Another is the long-term (active since 2002) Whim Bog experiment near Edinburg, Scotland (Sheppard *et al*., 2011; Levy *et al*., 2019), where the effects of enrichment upon a peatland by gaseous ammonia (NH_3) and wet-deposited ammonium (NH_4^+) and nitrate (NO_3^-) are compared. Analysis by Sutton *et al*. (2020) indicates that vegetation declined three times more quickly when exposed to gaseous ammonia and three times for ammonium than for a similar dose of nitrate.

A significant limitation of these studies in defining tipping points is that the long timescale necessary for critical transitions to occur in some cases typically exceeds the lifespan of most observational and experimental studies (Taranu *et al*., 2018; Lamentowicz *et al*., 2019). Therefore, further palaeoecological work across a more extensive range of sites or with multiple cores from within a single site may also advance our understanding of ecosystem tipping points in response to alkalinisation.

5. Conclusion

This study is the first to investigate the long-term impacts of alkaline emissions on a peatland over centennial timescales. It establishes the first threshold indicator values for ecosystem tipping points in response to alkalinisation. Our findings demonstrate that alkaline pollution has had a profound influence upon ecosystem development at Varudi for more than 750 years, with ecosystem succession following both low-level, sustained mineral soil enrichment due to agricultural activities and intensive fly-ash fallout sustained over 160 years. We find that an increase in pH of 0.2 to 0.3 (corresponding to, approximately, a two to threefold increase in alkalinity) is sufficient to trigger a critical ecosystem shift. These can lead to a long-term decline in carbon accumulation over long timescales, and such changes may be slow to recover or permanent, even if the point source of pollution is eliminated. Our results, while insightful, have limitations that underscore the need for additional experimental and palaeoecological research to assess peatland responses and resilience to alkalinisation across a range of spatial and temporal scales. This would allow a better understanding of the timescales required for peatland recovery and how these ecosystem transitions influence greenhouse gas dynamics from affected sites. Alkalinisation poses a growing threat to peatlands worldwide and is a developing challenge for the 21st century (Sutton *et al.,* 2020). As carbon-rich ecosystems, peatlands are important in future atmospheric greenhouse gas

https://doi.org/10.5194/egusphere-2025-1351
Preprint. Discussion started: 17 April 2025

concentrations. Understanding how peatlands will respond to future alkalisation is essential for predicting the role of peatlands in climate change mitigation.

6. Acknowledgements

The study was funded by the National Science Centre, Poland, grant no 2021/41/B/ST10/00060. We wish to thank the Estonian Research Council (projects PRG1993 and TK215) for providing additional financial support. Thanks to Eliise Kara, Merlin Liiv and Triin Reitalu for their assistance in the field.

Data availability statement:

All relevant data files described here are available either in the supplementary materials or via FigShare, accessible via the following link: https://figshare.com/s/acfe140783b6f871f1f2

Author contributions:

LOA prepared the manuscript with contributions from all authors. ML, MS and SV conceptualised the study and secured funding. LOA, ML, MS, KM, LA and NS participated in fieldwork. LA, SC, MB, ML, PK, MK, EŁ, AC and MAL conducted formal analyses. SV and AH provided historical data and photographs.

Declaration of interests:

The authors declare they have no known financial interests or personal relationships that could influence the work represented in this manuscript.

https://doi.org/10.5194/egusphere-2025-1351
Preprint. Discussion started: 17 April 2025

7. References

Abril, G.A., Wannaz, E.D., Mateos, A.C., Pignata, M.L., 2014. Biomonitoring of airborne particulate matter emitted from a cement plant and comparison with dispersion modelling results. *Atmos. Environ*. 82, 154–163. https://doi.org/10.1016/j.atmosenv.2013.10.020

Amesbury, M.J., Swindles, G.T., Bobrov, A., Charman, D.J., Holden, J., Lamentowicz, M., Mallon, G., Mazei, Y., Mitchell, E.A., Payne, R.J. and Roland, T.P., 2016. Development of a new pan-European testate amoeba transfer function for reconstructing peatland palaeohydrology. *Quat. Sci. Rev.*, *152*, pp.132-151. https://doi.org/10.1016/j.quascirev.2016.09.024

Apolinarska, K., Pleskot, K., Aunina, L., Marzec, M., Szczepaniak, M., Kabaciński, M., Kiełczewski, R. and Gałka, M., 2024. Late Holocene changes in the water table at an alkaline fen in Central Latvia: Their impacts on $CaCO_3$ deposition at the fen and relation to the hydroclimate patterns of the Eastern Baltic Region. *Quat. Sci. Rev.*, *334*, p.108717. https://doi.org/10.1016/j.quascirev.2024.108717

Appleby, P.G., 1998. *Dating recent sediments by 210 Pb: problems and solutions* (No. STUK-A--145).

Aquino-López, M.A., Blaauw, M., Christen, J.A. and Sanderson, N.K., 2018. Bayesian analysis of 210 Pb dating. *J. of Agric. Biol and Environ. Statistics*, *23*(3), pp.317-333. https://doi.org/10.1007/s13253-018-0328-7

Aquino-López, M.A., Ruiz-Fernández, A.C., Blaauw, M. and Sanchez-Cabeza, J.A., 2020. Comparing classical and Bayesian 210Pb dating models in human-impacted aquatic environments. *Quat. Geochronol.*, *60*, p.101106. https://doi.org/10.1016/j.quageo.2020.101106

Auber, A., Travers-Trolet, M., Villanueva, M.C. and Ernande, B., 2017. A new application of principal response curves for summarizing abrupt and cyclic shifts of communities over space. *Ecosphere*, *8*(12), p.e02023. https://doi.org/10.1002/ecs2.2023

Avel, E. and Pensa, M., 2013. Preparation of testate amoebae samples affects water table depth reconstructions in peatland palaeoecological studies. *Estonian J. of Earth Sci.*, *62*(2), p.113. doi:10.3176/earth.2013.09

Bacon, K.L., Baird, A.J., Blundell, A., Bourgault, M.A., Chapman, P.J., Dargie, G., Dooling, G.P., Gee, C., Holden, J., Kelly, T.J. and McKendrick-Smith, K.A., 2017. Questioning ten common assumptions about peatlands. *Mires and Peat*, *19*, pp.1-23.

https://doi.org/10.5194/egusphere-2025-1351
Preprint. Discussion started: 17 April 2025

907 Ball, D.F., 1964. Loss-on-ignition as an estimate of organic matter and organic carbon in non-
908 calcareous soils. *J. of Soil Sci.*, *15*(1), pp.84-92.
909 Barber, K.E., Battarbee, R.W., Brooks, S.J., Eglinton, G., Haworth, E.Y., Oldfield, F., Stevenson,
910 A.C., Thompson, R., Appleby, P.G., Austin, W.E.N. and Cameron, N.G., 1999. Proxy
911 records of climate change in the UK over the last two millennia: documented change
912 and sedimentary records from lakes and bogs. *J. of the Geol. Soc.*, *156*(2), pp.369-
913 380. https://doi.org/10.1144/gsjgs.156.2.0369
914 Barthelmes, A., de Klerk, P., Prager, A., Theuerkauf, M., Unterseher, M. and Joosten, H.,
915 2012. Expanding NPP analysis to eutrophic and forested sites: Significance of NPPs in
916 a Holocene wood peat section (NE Germany). *Rev. of Palaeobot. and Palynol.*, *186*,
917 pp.22-37. https://doi.org/10.1016/j.revpalbo.2012.07.007
918 Beck, K.K., Fletcher, M.S., Gadd, P.S., Heijnis, H., Saunders, K.M., Simpson, G.L. and Zawadzki,
919 A., 2018. Variance and rate-of-change as early warning signals for a critical transition
920 in an aquatic ecosystem state: a test case from Tasmania, Australia. *J. of Geophysical*
921 *Res.: Biogeosciences*, *123*(2), pp.495-508. https://doi.org/10.1002/2017JG004135
922 Berglund, B.E. and Ralska-Jasiewiczowa, M., 1986. Pollen analysis and pollen
923 diagrams. *Handbook of Holocene palaeoecology and palaeohydrology*, *455*, pp.484-
924 486.
925 Beug. H. J., 2009. Hans-Jürgen Beug, Leitfaden der Pollenbestimmung für Mitteleuropa und
926 angrenzende Gebiete. *Germania: Anzeiger der Römisch-Germanischen Kommission*
927 *des Deutschen Archäologischen Instituts*, pp.699-702.
928 Blaauw, M., Christen, J.A., Aquino-Lopez, M.A., Esquivel-Vazquez, J., Belding, T., Theiler, J.,
929 Gough, B., Karney, C. and Blaauw, M.M., 2021. Package 'rplum'.
930 Bobbink, R., Hornung, M. and Roelofs, J.G., 1998. The effects of air-borne nitrogen pollutants
931 on species diversity in natural and semi-natural European vegetation. *J. of*
932 *Ecol.*, *86*(5), pp.717-738. https://doi.org/10.1046/j.1365-2745.1998.8650717.x
933 Boës, X., Rydberg, J., Martinez-Cortizas, A., Bindler, R. and Renberg, I., 2011. Evaluation of
934 conservative lithogenic elements (Ti, Zr, Al, and Rb) to study anthropogenic element
935 enrichments in lake sediments. *J. of Paleolimnology*, *46*, pp.75-87.
936 https://doi.org/10.1007/s10933-011-9515-z
937 Boj˘nanský, V. and Fargašová, A., 2007. *Atlas of seeds and fruits of Central and East-*
938 *European flora: the Carpathian Mountains region*. Springer Science & Business
939 Media.

https://doi.org/10.5194/egusphere-2025-1351
Preprint. Discussion started: 17 April 2025

940 Bossew, P., 2013. Anthropogenic radionuclides in environmental samples from Fukushima
941 Prefecture. *Radiat Emerg Med*, *2*(1), pp.69-75.
942 Boyle, J.F., 2001. Inorganic geochemical methods in palaeolimnology. *Tracking*
943 *environmental change using lake sediments: physical and geochemical methods*,
944 pp.83-141. https://doi.org/10.1007/0-306-47670-3_5
945 Bridgham, S.D., Pastor, J., Dewey, B., Weltzin, J.F. and Updegraff, K., 2008. Rapid carbon
946 response of peatlands to climate change. *Ecology*, *89*(11), pp.3041-3048.
947 https://doi.org/10.1890/08-0279.1
948 Brown, A. and Pluskowski, A., 2011. Detecting the environmental impact of the Baltic
949 Crusades on a late-medieval (13th–15th century) frontier landscape: palynological
950 analysis from Malbork Castle and hinterland, Northern Poland. *J. of Archaeol.*
951 *Sci., 38*(8), pp.1957-1966. https://doi.org/10.1016/j.jas.2011.04.010
952 Burge, O.R., Richardson, S.J., Wood, J.R. and Wilmshurst, J.M., 2023. A guide to assess
953 distance from ecological baselines and change over time in palaeoecological
954 records. *The Holocene*, *33*(8), pp.905-917.
955 https://doi.org/10.1177/09596836231169986
956 Buttler, A., Bragazza, L., Laggoun-Défarge, F., Gogo, S., Toussaint, M.L., Lamentowicz, M.,
957 Chojnicki, B.H., Słowiński, M., Słowińska, S., Zielińska, M. and Reczuga, M., 2023.
958 Ericoid shrub encroachment shifts aboveground–belowground linkages in three
959 peatlands across Europe and Western Siberia. *Global Change Biology*, *29*(23),
960 pp.6772-6793. https://doi.org/10.1111/gcb.16904
961 Chambers, F.M., Beilman, D.W. and Yu, Z., 2011. Methods for determining peat humification
962 and for quantifying peat bulk density, organic matter and carbon content for
963 palaeostudies of climate and peatland carbon dynamics. *Mires and Peat*, *7*(7), pp.1-
964 10.
965 Charman, D.J., 2001. Biostratigraphic and palaeoenvironmental applications of testate
966 amoebae. *Quat. Sci. Rev.*, *20*(16-17), pp.1753-1764. https://doi.org/10.1016/S0277-
967 3791(01)00036-1
968 Clymo, R.S., Turunen, J. and Tolonen, K., 1998. Carbon accumulation in peatland. *Oikos*,
969 pp.368-388. https://doi.org/10.2307/3547057
970 Cwanek, A., Łokas, E., Mitchell, E.A., Mazei, Y., Gaca, P. and Milton, J.A., 2021. Temporal
971 variability of Pu signatures in a 210Pb-dated Sphagnum peat profile from the

https://doi.org/10.5194/egusphere-2025-1351
Preprint. Discussion started: 17 April 2025

Northern Ural, Russian Federation. *Chemosphere*, *281*, p.130962. https://doi.org/10.1016/j.chemosphere.2021.13096

De'ath, G., 1999. Principal curves: a new technique for indirect and direct gradient analysis. *Ecology*, *80*(7), pp.2237-2253. https://doi.org/10.1890/0012-9658(1999)080[2237:PCANTF]2.0.CO;2

Dean, W.E., 1974. Determination of carbonate and organic matter in calcareous sediments and sedimentary rocks by loss on ignition; comparison with other methods. *J. of Sediment. Res.*, *44*(1), pp.242-248. https://doi.org/10.1306/74d729d2-2b21-11d7-8648000102c1865d

Defrenne, C.E., Moore, J.A., Tucker, C.L., Lamit, L.J., Kane, E.S., Kolka, R.K., Chimner, R.A., Keller, J.K. and Lilleskov, E.A., 2023. Peat loss collocates with a threshold in plant–mycorrhizal associations in drained peatlands encroached by trees. *New Phytologist*, *240*(1), pp.412-425. https://doi.org/10.1111/nph.18954

Dieleman, C.M., Branfireun, B.A., McLaughlin, J.W. and Lindo, Z., 2015. Climate change drives a shift in peatland ecosystem plant community: implications for ecosystem function and stability. *Glob. Change Biol.*, *21*(1), pp.388-395. DOI: 10.1111/gcb.12643

Favre, E., Escarguel, G., Suc, J.P., Vidal, G. and Thévenod, L., 2008. A contribution to deciphering the meaning of AP/NAP with respect to vegetation cover. *Review of Palaeobot. and Palynol.*, *148*(1), pp.13-35. https://doi.org/10.1016/j.revpalbo.2007.08.003

Fiałkiewicz-Kozieł, B., De Vleeschouwer, F., Mattielli, N., Fagel, N., Palowski, B., Pazdur, A. and Smieja-Król, B., 2018. Record of Anthropocene pollution sources of lead in disturbed peatlands from Southern Poland. *Atmos. Environm.*, *179*, pp.61-68 https://doi.org/10.1016/j.atmosenv.2018.02.002

Finsinger, W. and Tinner, W., 2005. Minimum count sums for charcoal concentration estimates in pollen slides: accuracy and potential errors. *The Holocene*, *15*(2), pp.293-297. https://doi.org/10.3389/fevo.2018.00149

Frolking, S., Roulet, N., Fuglestvedt, J., 2006. How northern peatlands influence the Earth's radiative budget: Sustained methane emission versus sustained carbon sequestration. *J. Geophys. Res. Biogeosciences* 111. https://doi.org/10.1029/2005JG000091

https://doi.org/10.5194/egusphere-2025-1351
Preprint. Discussion started: 17 April 2025

Goh, T.K., Ho, W.H., Hyde, K.D. and Umali, T.E., 1997. New records and species of Sporoschisma and Sporoschismopsis from submerged wood in the tropics. *Mycological research*, *101*(11), pp.1295-1307. https://doi.org/10.1017/S0953756297003973

Gomes, H.I., Mayes, W.M., Rogerson, M., Stewart, D.I. and Burke, I.T., 2016. Alkaline residues and the environment: a review of impacts, management practices and opportunities. *J. of Clean. Prod.*, *112*, pp.3571-3582. https://doi.org/10.1016/j.jclepro.2015.09.111

Gorham, E., 1991. Northern peatlands: role in the carbon cycle and probable responses to climatic warming. *Ecolog. Appl.*, *1*(2), pp.182-195. https://doi.org/10.2307/1941811

Graf, M.D., Rochefort, L. and Poulin, M., 2008. Spontaneous revegetation of cutwaway peatlands of North America. *Wetlands*, *28*, pp.28-39. https://doi.org/10.1672/06-136.1

Grimm, E.C., 1987. CONISS: a FORTRAN 77 program for stratigraphically constrained cluster analysis by the method of incremental sum of squares. *Computers & Geosci.*, *13*(1), pp.13-35. https://doi.org/10.1016/0098-3004(87)90022-7

Grosse-Brauckmann, G. 1972. *Über pflanzliche Makrofossilien mitteleuropäischer Torfe. I. Gewebereste krautiger Pflanzen und ihre Merkmale* (On plant macrofossils in central European peat. I. Remnants of vascular plant tissues and their characteristics). *Telma*, 2, 19 55 (in German).

Grosse-Brauckmann, G. 1974. *Über pflanzliche Makrofossilien mitteleuropäischer Torfe. II. Weitere Reste (Früchte und Samen, Moose u.a.) und ihre Bestimmungsmöglichkeiten* (On plant macrofossils in central European peat. II. Other remnants (e.g. fruits and seeds, mosses) and possibilities for their identification). *Telma*, 4, 51–117 (in German).

Gunnarsson, U., Malmer, N. and Rydin, H., 2002. Dynamics or constancy in Sphagnum dominated mire ecosystems? A 40-year study. *Ecography*, *25*(6), pp.685-704. https://doi.org/10.1034/j.1600-0587.2002.250605.x

Hájek, M., Horsák, M., Hájková, P. and Dítě, D., 2006. Habitat diversity of central European fens in relation to environmental gradients and an effort to standardise fen terminology in ecological studies. *Perspect. Plant Ecol, Evol. and Syst.*, *8*(2), pp.97-114. https://doi.org/10.1016/j.ppees.2006.08.002

https://doi.org/10.5194/egusphere-2025-1351
Preprint. Discussion started: 17 April 2025

Hájek, M., Hájková, P., Apostolova, I., Sopotlieva, D., Goia, I., Dítě, D., 2021. The vegetation of rich fens (Sphagno warnstorfii-Tomentypnion nitentis) at the southeastern margins of their European range. *Veg. Class. and Surv. 2*, 177–190. https://doi.org/10.3897/vcs/2021/69118

Harenda, K.M., Lamentowicz, M., Samson, M., Chojnicki, B.H., 2018. The Role of Peatlands and Their Carbon Storage Function in the Context of Climate Change, in: Zielinski, T., Sagan, I., Surosz, W. (Eds.), *Interdisciplinary Approaches for Sustainable Development Goals: Economic Growth, Social Inclusion and Environmental Protection*. Springer International Publishing, Cham, pp. 169–187. https://doi.org/10.1007/978-3-319-71788-3_12

Heidelberg Materials Kunda AS (2023) Heidelberg Materials Kunda AS. Available at: https://www.kunda.heidelbergmaterials.ee/et/tegevusandmed (Accessed: 24 February 2025).

Heinsalu, A., Veski, S., 2010. Palaeoecological evidence of agricultural activity and human impact on the environment at the ancient settlement centre of Keava, Estonia. *Estonian Journal of Earth Sciences*, 59, pp.80-89. doi: 10.3176/earth.2010.1.06

Hendon, D. and Charman, D.J., 1997. The preparation of testate amoebae (Protozoa: Rhizopoda) samples from peat. *The Holocene*, *7*(2), pp.199-205. https://doi.org/10.1177/095968369700700207

Hendon, D., Charman, D.J. and Kent, M., 2001. Palaeohydrological records derived from testate amoebae analysis from peatlands in northern England: within-site variability, between-site comparability and palaeoclimatic implications. *The Holocene*, *11*(2), pp.127-148. https://doi.org/10.1191/095968301674575645

Ivanov, Y.V., Kartashov, A.V., Ivanova, A.I., Ivanov, V.P., Marchenko, S.I., Nartov, D.I., Kuznetsov, V.V., 2018. Long-term impact of cement plant emissions on the elemental composition of both soils and pine stands and on the formation of Scots pine seeds. *Environ. Pollut*. 243, 1383–1393. https://doi.org/10.1016/j.envpol.2018.09.099

Jalkanen *et al.,* 2000 The effect of large anthropogenic particulate emissions on atmospheric aerosols deposition and bioindicators in the eastern Gulf of Finland region.

Jalkanen, L., Mäkinen, A., Häsänen, E. and Juhanoja, J., 2000. The effect of large anthropogenic particulate emissions on atmospheric aerosols, deposition and bioindicators in the eastern Gulf of Finland region. *Sci. of the Total Env.*, *262*(1-2), pp.123-136. https://doi.org/10.1016/S0048-9697(00)00602-1

https://doi.org/10.5194/egusphere-2025-1351
Preprint. Discussion started: 17 April 2025

Joosten, H. and Clarke, D., 2002. Wise use of mires and peatlands. *International mire conservation group and international peat society*, *304*.

Joosten, H., 2003. Wise use of mires: Background and principles 239–250.

Juggins, S. and Juggins, M.S., 2019. Package 'rioja'.

Kaasik, A., Kont, R. and Lõhmus, A., 2023. Modeling forest landscape futures: Full scale simulation of realistic socioeconomic scenarios in Estonia. *Plos one*, *18*(11), p.e0294650. 10.2495/GEO080171

Kaasik, M., Liblik, V. and Kaasik, H., 1999. Long-term deposition patterns of airborne wastes in the North-East of Estonia. *Oil Shale*, *16*(4), pp.315-330. DOI: 10.3176/oil.1999.4.04

Kang, H., Kwon, M.J., Kim, S., Lee, S., Jones, T.G., Johncock, A.C., Haraguchi, A. and Freeman, C., 2018. Biologically driven DOC release from peatlands during recovery from acidification. *Nature communications*, *9*(1), p.3807. https://doi.org/10.1038/s41467-018-06259-1

Karofeld, E., 1996. The effects of alkaline fly ash precipitation on the Sphagnum mosses in Niinsaare bog, NE Estonia. *Suoseura - Finnish Peatland Society* Helsinki

Kask, R., Ots, K., Mandre, M., Pikk, J., 2008. Scots pine (Pinus sylvestris L.) wood properties in an alkaline air pollution environment. *Trees* 22, 815–823. https://doi.org/10.1007/s00468-008-0242-7

Katz, N.J., Katz, S.V. & Skobeyeva, E.I. 1977. *Atlas Rastitel'nyh Oostatkov v Torfje* (*Atlas of Plant Remains in Peats*). Nedra, Moscow, 736pp. (in Russian)

Katz, N.J., Katz, S.V. and Kipiani, M.G., 1965. *Atlas and keys of fruits and seeds occurring in the Quaternary deposits of the USSR*. Publishing House Nauka, Moscow.

Keppler, F., Eiden, R., Niedan, V., Pracht, J. and Schöler, H.F., 2000. Halocarbons produced by natural oxidation processes during degradation of organic matter. *Nature*, *403*(6767), pp.298-301. https://doi.org/10.1038/35002055

Ketterer, M.E., Hafer, K.M. and Mietelski, J.W., 2004. Resolving Chernobyl vs. global fallout contributions in soils from Poland using Plutonium atom ratios measured by inductively coupled plasma mass spectrometry. *J. of Env. Radioact.*, *73*(2), pp.183-201. https://doi.org/10.1016/j.jenvrad.2003.09.001

Klõšeiko, J., Kuznetsova, T., Tilk, M. and Mandre, M., 2014. Short-term influence of Clinker dust and wood ash on macronutrients and growth in Norway spruce (Picea abies) and Scots pine (Pinus sylvestris) seedlings. *Commun in Soil Sci and Plant Analysis*, *45*(16), pp.2105-2117. https://doi.org/10.1080/00103624.2014.929695

https://doi.org/10.5194/egusphere-2025-1351
Preprint. Discussion started: 17 April 2025

Koff, T., Vandel, E., Marzecová, A., Avi, E. and Mikomägi, A., 2016. Assessment of the effect of anthropogenic pollution on the ecology of small shallow lakes using the palaeolimnological approach. *Estonian J. of Earth Sci.*, *65*(4). Doi: 10.3176/earth.2016.19

Konings, W., Boyd, K. and Andersen, R., 2019. Comparison of plant traits of sedges, shrubs and Sphagnum mosses between sites undergoing forest-to-bog restoration and near-natural open blanket bog: a pilot study. *Mires and Peat*, *23*, pp.1-10.

Korhola, A., Tolonen, K., Turunen, J. and Jungner, H., 1995. Estimating long-term carbon accumulation rates in boreal peatlands by radiocarbon dating. *Radiocarbon*, *37*(2), pp.575-584. 995;37(2) doi:10.1017/S0033822200031064

Kuhry, P., 1985. Transgression of a raised bog across a coversand ridge originally covered with an oak—lime forest: palaeoecological study of a middle holocene local vegetational succession in the Amtsven (Northwest Germany). *Rev. of Palaeobot. and Palynol.*, *44*(3-4), pp.303-353. https://doi.org/10.1016/0034-6667(85)90023-5

Kuhry, P., 1997. The palaeoecology of a treed bog in western boreal Canada: a study based on microfossils, macrofossils and physico-chemical properties. *Rev. of Palaeobot. and Palynol*, *96*(1-2), pp.183-224. https://doi.org/10.1016/S0034-6667(96)00018-8

Lamentowicz, M., Gałka, M., Marcisz, K., Słowiński, M., Kajukało-Drygalska, K., Dayras, M.D. and Jassey, V.E., 2019. Unveiling tipping points in long-term ecological records from Sphagnum-dominated peatlands. *Biol. Lett.*, *15*(4), p.20190043. https://doi.org/10.1098/rsbl.2019.0043

Lee-Taylor, J.M. and Holland, E.A., 2000. Litter decomposition as a potential natural source of methyl bromide. *J. of Geophys. Res.: Atmos.*, *105*(D7), pp.8857-8864. https://doi.org/10.1029/1999JD901112

Lehmann, N., Lantuit, H., Böttcher, M.E., Hartmann, J., Eulenburg, A., Thomas, H., 2023. Alkalinity generation from carbonate weathering in a silicate-dominated headwater catchment at Iskorasfjellet, northern Norway. *Biogeosciences* 20, 3459–3479. https://doi.org/10.5194/bg-20-3459-2023

Leifeld, J. and Menichetti, L., 2018. The underappreciated potential of peatlands in global climate change mitigation strategies. *Nature Commun.*, *9*(1), p.1071. https://doi.org/10.1038/s41467-018-03406-6

Levy, P., van Dijk, N., Gray, A., Sutton, M., Jones, M., Leeson, S., Dise, N., Leith, I. and Sheppard, L., 2019. Response of a peat bog vegetation community to long-term

https://doi.org/10.5194/egusphere-2025-1351
Preprint. Discussion started: 17 April 2025

experimental addition of nitrogen. *J. of Ecol.*, *107*(3), pp.1167-1186. https://doi.org/10.1111/1365-2745.13107

Liblik, V., Rätsep, A. and Kundel, H., 1995. Pollution sources and spreading of sulphur dioxide in the North-Eastern Estonia. *Water, Air, and Soil Pollut.*, *85*, pp.1903-1908. https://doi.org/10.1007/BF01186112

Liiv, S. and Kaasik, M., 2004. Trace metals in mosses in the Estonian oil shale processing region. *J. of Atmos. Chemistry*, *49*, pp.563-578. https://doi.org/10.1007/s10874-004-1266-z

Limpens, J., Berendse, F. and Klees, H., 2003. N deposition affects N availability in interstitial water, growth of Sphagnum and invasion of vascular plants in bog vegetation. *New Phytologist*, *157*(2), pp.339-347. https://doi.org/10.1046/j.1469-8137.2003.00667.x

Liu, B., Heinemeyer, A., Marchant, R. and Mills, R.T., 2024. Exploring optimal sampling strategy of testate amoebae as hydrological bioindicators in UK upland peatlands. *J. of Env. Manag.*, *370*, p.122959. https://doi.org/10.1016/j.jenvman.2024.122959

Loisel, J. and Bunsen, M., 2020. Abrupt fen-bog transition across southern Patagonia: Timing, causes, and impacts on carbon sequestration. *Front. in Ecol. and Evol.*, *8*, p.273. https://doi.org/10.3389/fevo.2020.00273

Longman, J., Veres, D. and Wennrich, V., 2019. Utilisation of XRF core scanning on peat and other highly organic sediments. *Quat. Int.*, *514*, pp.85-96. https://doi.org/10.1016/j.quaint.2018.10.015

Łuców, D., Küttim, M., Słowiński, M., Kołaczek, P., Karpińska-Kołaczek, M., Küttim, L., Salme, M. and Lamentowicz, M., 2022. Searching for an ecological baseline: Long-term ecology of a post-extraction restored bog in Northern Estonia. *Quat. Int.*, *607*, pp.65-78. https://doi.org/10.1016/j.quaint.2021.08.017

Maimer, N., Horton, D.G. and Vitt, D.H., 1992. Element concentrations in mosses and surface waters of western Canadian mires relative to precipitation chemistry and hydrology. *Ecography*, *15*(1), pp.114-128. https://doi.org/10.1111/j.1600-0587.1992.tb00015.x

Mandre, M. and Korsjukov, R., 2007. The quality of stemwood of Pinus sylvestris in an alkalised environment. *Water, air, and soil pollution*, *182*, pp.163-172. https://doi.org/10.1007/s11270-006-9329-1

https://doi.org/10.5194/egusphere-2025-1351
Preprint. Discussion started: 17 April 2025

Mandre, M. and Ots, K., 1999. Growth and biomass partitioning of 6-year-old spruces under alkaline dust impact. *Water, Air, and Soil Poll.*, *114*, pp.13-25. https://doi.org/10.1023/A:1005048921852

Marcisz, K., Jassey, V.E., Kosakyan, A., Krashevska, V., Lahr, D.J., Lara, E., Lamentowicz, Ł., Lamentowicz, M., Macumber, A., Mazei, Y. and Mitchell, E.A., 2020. Testate amoeba functional traits and their use in paleoecology. *Front. in Ecol. and Evol., 8*, p.575966. https://doi.org/10.3389/fevo.2020.575966

Mauquoy, D and van Geel, B., 2007. Mire and peat macros. *Encyclopedia Quaternary Science*, *3*, pp.2315-2336.

Mauquoy, D., Hughes, P.D.M. and Van Geel, B., 2010. A protocol for plant macrofossil analysis of peat deposits. *Mires and Peat*, *7*(6), pp.1-5.

Mazei and Tsyganov, 2006. *Freshwater testate amoebae* [in Russian], KMK Scientific pressSBN: 5-87317-336-2

Mitchell, E.A., Charman, D.J. and Warner, B.G., 2008. Testate amoebae analysis in ecological and paleoecological studies of wetlands: past, present and future. *Biodivers. and Conserv. 17*, pp.2115-2137. https://doi.org/10.1007/s10531-007-9221-3

Moore, P.D., Webb, J.A. and Collison, M.E., 1991. *Pollen analysis* (pp. viii+-216).

Mróz, T., Łokas, E., Kocurek, J. and Gąsiorek, M., 2017. Atmospheric fallout radionuclides in peatland from Southern Poland. *J. of Envi. Radioact.*, *175*, pp.25-33 https://doi.org/10.1016/j.jenvrad.2017.04.012

Munson, S.M., Reed, S.C., Peñuelas, J., McDowell, N.G. and Sala, O.E., 2018. Ecosystem thresholds, tipping points, and critical transitions. *New Phytologist*, *218*(4), pp.1315-1317. https://www.jstor.org/stable/90021529

Niinemets, E. and Saarse, L., 2009. Holocene vegetation and land-use dynamics of south-eastern Estonia. *Quat Int.*, *207*(1-2), pp.104-116. https://doi.org/10.1016/j.quaint.2008.11.015

Oksanen, J., Blanchet, F.G., Kindt, R., Legendre, P., Minchin, P.R., O'hara, R.B., Simpson, G.L., Solymos, P., Stevens, M.H.H., Wagner, H. and Oksanen, M.J., 2019. Package 'vegan'. *Community ecology package, version*, *2*(9), pp.1-295.

Orme, L.C., Davies, S.J. and Duller, G.A.T., 2015. Reconstructed centennial variability of late Holocene storminess from Cors Fochno, Wales, UK. *J. of Quat. Sci.*, *30*(5), pp.478-488. https://doi.org/10.1002/jqs.2792

https://doi.org/10.5194/egusphere-2025-1351
Preprint. Discussion started: 17 April 2025

Órpez, R., Martínez, M.E., Hodaifa, G., El Yousfi, F., Jbari, N. and Sánchez, S., 2009. Growth of the microalga Botryococcus braunii in secondarily treated sewage. *Desalination*, *246*(1-3), pp.625-630. https://doi.org/10.1016/j.desal.2008.07.016

Osborne, C., Gilbert-Parkes, S., Spiers, G., Lamit, L.J., Lilleskov, E.A., Basiliko, N., Watmough, S., Andersen, R., Artz, R.E., Benscoter, B.W., Bragazza, L., Bräuer, S.L., Carson, M.A., Chen, X., Chimner, R.A., Clarkson, B.R., Enriquez, A.S., Grover, S.P., Harris, L.I., Hazard, C., Hribljan, J., Juutinen, S., Kane, E.S., Knorr, K.-H., Kolka, R., Laine, A.M., Larmola, T., McCalley, C.K., McLaughlin, J., Moore, T.R., Mykytczuk, N., Normand, A.E., Olefeldt, D., Rich, V., Roulet, N., Rupp, D.L., Rutherford, J., Schadt, C.W., Sonnentag, O., Tedersoo, L., Trettin, C.C., Tuittila, E.-S., Turetsky, M., Urbanová, Z., Varner, R.K., Waldrop, M.P., Wang, M., Wang, Z., Wiedermann, M.M., Williams, S.T., Yavitt, J.B., Yu, Z.-G., Global Peatland Microbiome Project, 2024. Global Patterns of Metal and Other Element Enrichment in Bog and Fen Peatlands. *Arch. Environ. Contam. Toxicol*. 86, 125–139. https://doi.org/10.1007/s00244-024-01051-3

Osterkamp, T.E., Viereck, L., Shur, Y., Jorgenson, M.T., Racine, C., Doyle, A. and Boone, R.D., 2000. Observations of thermokarst and its impact on boreal forests in Alaska, USA. *Arctic, Antarctic, and Alpine Res.*, *32*(3), pp.303-315. https://doi.org/10.1080/15230430.2000.12003368

Ots, K. and Mandre, M., 2012. Monitoring of heavy metals uptake and allocation in Pinus sylvestris organs in alkalised soil. *Env. Monit. and Assess.*, *184*, pp.4105-4117. https://doi.org/10.1007/s10661-011-2247-8

Ots, K. and Reisner, V., 2006. Scots pine (Pinus sylvestris L.) and its habitat in Muraka bog under the influence of wastes from the Narva power plants (North-East Estonia). *Proc. Estonian Acad. Sci. Biol. Ecol*, *55*(2), pp.137-148.

Ots, K., Tilk, M. and Aguraijuja, K., 2017. The effect of oil shale ash and mixtures of wood ash and oil shale ash on the above-and belowground biomass formation of Silver birch and Scots pine seedlings on a cutaway peatland. *Eco. Eng. 108*, pp.296-306. https://doi.org/10.1016/j.ecoleng.2017.09.002

Paal, J., Vellak, K., Liira, J. and Karofeld, E., 2010. Bog recovery in northeastern Estonia after the reduction of atmospheric pollutant input. *Restor. Eco.*, *18*, pp.387-400. https://doi.org/10.1111/j.1526-100X.2009.00608.x

https://doi.org/10.5194/egusphere-2025-1351
Preprint. Discussion started: 17 April 2025

Pärtel, M., Helm, A., Ingerpuu, N., Reier, Ü. and Tuvi, E.L., 2004. Conservation of Northern European plant diversity: the correspondence with soil pH. *Biol. Conserv.*, *120*(4), pp.525-531. https://doi.org/10.1016/j.biocon.2004.03.025

Pärtma, M. 2023. *The recovery of bogs in NE-Estonia bogs from alkaline air pollution. Case study of Varudi, Sämi-Kurustiku and Uljaste bogs*. Master Thesis, Tallinn University. 97 pp. (in Estonian with English summary).

Patterson III, W.A., Edwards, K.J., Maguire, D.J., 1987. Microscopic charcoal as a fossil indicator of fire. *Quat. Sci. Rev*. 6, 3–23. https://doi.org/10.1016/0277-3791(87)90012-6

Payne, R.J. and Mitchell, E.A., 2009. How many is enough? Determining optimal count totals for ecological and palaeoecological studies of testate amoebae. *J. of Paleolimnology*, *42*(4), pp.483-495. https://doi.org/10.1007/s10933-008-9299-y

Pensa, M., Jalkanen, R. and Liblik, V., 2007. Variation in Scots pine needle longevity and nutrient conservation in different habitats and latitudes. *Canadian J. of For. Res. 37*(9), pp.1599-1604. https://doi.org/10.1139/X07-012

Pensa, M., Liblik, V. and Jalkanen, R., 2004. Temporal changes in the state of a pine stand in a bog affected by air pollution in northeast Estonia. *Water, Air, and Soil Poll*, *159*, pp.87-99. https://doi.org/10.1023/B:WATE.0000049191.36830.a7

Piotrowska, N., Blaauw, M., Mauquoy, D. and Chambers, F.M., 2011. Constructing deposition chronologies for peat deposits using radiocarbon dating. *Mires and Peat*, *7*(10), pp.1-14.

Poska, A. and Saarse, L., 2002. Vegetation development and introduction of agriculture to Saaremaa Island, Estonia: the human response to shore displacement. *The Holocene*, *12*(5), pp.555-568. https://doi.org/10.1191/0959683602hl567rp

Poska, A., 2003. *Human impact on vegetation of coastal Estonia during the Stone Age*. Doctoral Dissertation, Uppsala Universitet, Sweden.

R Core Team (2023). R: A Language and Environment for Statistical Computing. R Foundation for Statistical Computing, Vienna, Austria. <https://www.R-project.org/>.

Raukas, A. (ed.). 1993. Environmental Impact Assessment for the Area of Influence of Reconstructed Kunda Cement Factory. Present Situation and Prediction of Potential Changes. Tallinn (manuscript).

https://doi.org/10.5194/egusphere-2025-1351
Preprint. Discussion started: 17 April 2025

Rawlins, A. and Morris, J., 2010. Social and economic aspects of peatland management in Northern Europe, with particular reference to the English case. *Geoderma*, *154*(3-4), pp.242-251. https://doi.org/10.1016/j.geoderma.2009.02.022

Reimer, P.J., Austin, W.E., Bard, E., Bayliss, A., Blackwell, P.G., Ramsey, C.B., Butzin, M., Cheng, H., Edwards, R.L., Friedrich, M. and Grootes, P.M., 2020. The IntCal20 Northern Hemisphere radiocarbon age calibration curve (0–55 cal kBP). *Radiocarbon*, *62*(4), pp.725-757. https://doi.org/10.1017/RDC.2020.41

Roderfeld, H., 1993. *Raised bog regeneration after peat harvesting in north-west Germany.*

Roulet, N.T., Lafleur, P.M., Richard, P.J., Moore, T.R., Humphreys, E.R. and Bubier, J.I.L.L., 2007. Contemporary carbon balance and late Holocene carbon accumulation in a northern peatland. *Glob. Change Biol.*, *13*(2), pp.397-411. https://doi.org/10.1111/j.1365-2486.2006.01292.x

Schindler, D.W., 1997. Widespread effects of climatic warming on freshwater ecosystems in North America. *Hydrol. Process.*, *11*(8), pp.1043-1067. https://doi.org/10.1002/(SICI)1099-1085(19970630)11:8<1043::AID-HYP517>3.0.CO;2-5

Seppä, H. and Bennett, K.D., 2003. Quaternary pollen analysis: recent progress in palaeoecology and palaeoclimatology. *Prog. in Phys. Geog.*, *27*(4), pp.548-579. https://doi.org/10.1191/0309133303pp394oa

Sheppard, L.J., Leith, I.D., Mizunuma, T., Neil Cape, J., Crossley, A., Leeson, S., Sutton, M.A., van Dijk, N. and Fowler, D., 2011. Dry deposition of ammonia gas drives species change faster than wet deposition of ammonium ions: Evidence from a long-term field manipulation. *Glob. Change Biol.*, *17*(12), pp.3589-3607. https://doi.org/10.1111/j.1365-2486.2011.02478.x

Shotyk, W., 1997. Atmospheric deposition and mass balance of major and trace elements in two oceanic peat bog profiles, northern Scotland and the Shetland Islands. *Chem. Geol. 138*(1-2), pp.55-72. https://doi.org/10.1016/S0009-2541(96)00172-6

Sibul, I., Plado, J. and Jõeleht, A., 2017. Ground-penetrating radar and electrical resistivity tomography for mapping bedrock topography and fracture zones: a case study in Viru-Nigula, NE Estonia. *Estonian J. of Earth Sci.*, *66*(3), p.142. https://doi.org/10.3176/earth.2017.11

Siemensma, F., (2019). *Microworld – world of amoeboid organisms.* [online] Arcella.nl. Available at: < https://arcella.nl > (accessed 10/2023)

https://doi.org/10.5194/egusphere-2025-1351
Preprint. Discussion started: 17 April 2025

Silva-Sánchez, N., Martínez Cortizas, A. and López-Merino, L., 2014. Linking forest cover, soil erosion and mire hydrology to late-Holocene human activity and climate in NW Spain. *The Holocene*, *24*(6), pp.714-725. https://doi.org/10.1177/0959683614526934

Simpson, G.L., 2018. Modelling palaeoecological time series using generalised additive models. *Front. Ecol. Evol*, *6*, p.149. https://doi.org/10.3389/fevo.2018.00149

Simpson, G.L., Oksanen, J. and Simpson, M.G.L., 2016. Package 'analogue'. *Analogue and Weighted Averaging Methods for Palaeoecology*.

Stelling, J.M., Slesak, R.A., Windmuller-Campione, M.A. and Grinde, A., 2023. Effects of stand age, tree species, and climate on water table fluctuations and estimated evapotranspiration in managed peatland forests. *J. of Env. Management*, *339*, p.117783. https://doi.org/10.1016/j.jenvman.2023.117783

Stockmarr, J., 1971. Tables with spores used in absolute pollen analysis. *Pollen et spores*, *13*, pp.615-621.

Sutton, M.A., van Dijk, N., Levy, P.E., Jones, M.R., Leith, I.D., Sheppard, L.J., Leeson, S., Sim Tang, Y., Stephens, A., Braban, C.F., Dragosits, U., Howard, C.M., Vieno, M., Fowler, D., Corbett, P., Naikoo, M.I., Munzi, S., Ellis, C.J., Chatterjee, S., Steadman, C.E., Móring, A., Wolseley, P.A., 2020. Alkaline air: changing perspectives on nitrogen and air pollution in an ammonia-rich world. *Philos. Trans. R. Soc. Math. Phys. Eng. Sci*. 378, 20190315. https://doi.org/10.1098/rsta.2019.0315

Swindles, G.T., 2010. Dating recent peat profiles using spheroidal carbonaceous particles (SCPs). *Mires and peat*, 7.

Szumigalski, A.R. and Bayley, S.E., 1996. Decomposition along a bog to rich fen gradient in central Alberta, Canada. *Canadian J. of Bot.*, *74*(4), pp.573-581. https://doi.org/10.1139/b96-073

Tanneberger, F., Moen, A., Barthelmes, A., Lewis, E., Miles, L., Sirin, A., Tegetmeyer, C. and Joosten, H., 2021. Mires in Europe—Regional diversity, condition and protection. *Diversity*, *13*(8), p.381. https://doi.org/10.3390/d13080381

Taranu, Z.E., Carpenter, S.R., Frossard, V., Jenny, J.P., Thomas, Z., Vermaire, J.C. and Perga, M.E., 2018. Can we detect ecosystem critical transitions and signals of changing resilience from paleo-ecological records?. *Ecosphere*, *9*(10), p.e02438. https://doi.org/10.1002/ecs2.2438

https://doi.org/10.5194/egusphere-2025-1351
Preprint. Discussion started: 17 April 2025

Thormann, M.N., Currah, R.S. and Bayley, S.E., 2003. Succession of microfungal assemblages in decomposing peatland plants. *Plant and Soil*, *250*, pp.323-333. https://doi.org/10.1023/A:1022845604385

Tobolski, K., 2000. Przewodnik do oznaczania torfów i osadów jeziornych [Guide to the determination of peat and lake sediments, in Polish]. Vademecum Geobotanicum. T. 2. *Warszawa. Wydaw. Nauk. PWN*, p.508.

Trumm, U., Raju, T. and Kangur, P., 2010. Kunda tsement - 140: tsemendi tootmise ajalugu Kundas 1870-2010. In *Nomine OÜ, Tallinn*. (in Estonian).

Turetsky, M.R. and St. Louis, V.L., 2006. Disturbance in boreal peatlands. In *Boreal peatland ecosystems* (pp. 359-379). Berlin, Heidelberg: Springer Berlin Heidelberg.

Turner, T.E., Swindles, G.T. and Roucoux, K.H., 2014. Late Holocene ecohydrological and carbon dynamics of a UK raised bog: impact of human activity and climate change. *Quat. Sci. Rev.*, *84*, pp.65-85. https://doi.org/10.1016/j.quascirev.2013.10.030

Uno, K.T., Quade, J., Fisher, D.C., Wittemyer, G., Douglas-Hamilton, I., Andanje, S., Omondi, P., Litoroh, M. and Cerling, T.E., 2013. Bomb-curve radiocarbon measurement of recent biologic tissues and applications to wildlife forensics and stable isotope (paleo) ecology. *Proc. of the Nat. Acad. of Sci.*, *110*(29), pp.11736-11741. https://doi.org/10.1073/pnas.1302226110

Vaasma, T., Kaasik, M., Loosaar, J., Kiisk, M. and Tkaczyk, A.H., 2017. Long-term modelling of fly ash and radionuclide emissions as well as deposition fluxes due to the operation of large oil shale-fired power plants. *J. of Env. Radioact*, *178*, pp.232-244. https://doi.org/10.1016/j.jenvrad.2017.08.017

Vaasma, T., Kiisk, M., Meriste, T. and Tkaczyk, A.H., 2014. The enrichment of natural radionuclides in oil shale-fired power plants in Estonia–The impact of new circulating fluidized bed technology. *J. of Env. Radioact*, *129*, pp.133-139. https://doi.org/10.1016/j.jenvrad.2014.01.002

Van den Brink, P.J. and Braak, C.J.T., 1999. Principal response curves: Analysis of time-dependent multivariate responses of biological community to stress. *Env. Toxico. and Chemistry: An Int. J.* *18*(2), pp.138-148. https://doi.org/10.1002/etc.5620180207

van Geel, B. and Aptroot, A., 2006. Fossil ascomycetes in Quaternary deposits. *Nova Hedwigia*, *82*(3), pp.313-330. https://hdl.handle.net/11245/1.255775

https://doi.org/10.5194/egusphere-2025-1351
Preprint. Discussion started: 17 April 2025

Van Geel, B., 1978. A palaeoecological study of Holocene peat bog sections in Germany and the Netherlands, based on the analysis of pollen, spores and macro-and microscopic remains of fungi, algae, cormophytes and animals. *Rev of palaeobot and palynol., 25*(1), pp.1-120. https://doi.org/10.1016/0034-6667(78)90040-4

Vandel, E. and Vaasma, T., 2018. Development of small lakes in Estonia: paleolimnological studies. *Dynamiques environnementales. J. Int. de géosciences et de l'environnement*, (42), pp.368-375. https://doi.org/10.4000/dynenviron.2533

Varvas, M. and Punning, J.M., 1993. Use of the 210Pb method in studies of the development and human-impact history of some Estonian lakes. *The Holocene*, *3*(1), pp.34-44. https://doi.org/10.1177/095968369300300104

Vellak, K., Liira, J., Karofeld, E., Galanina, O., Noskova, M. and Paal, J., 2014. Drastic turnover of bryophyte vegetation on bog microforms initiated by air pollution in Northeastern Estonia and bordering Russia. *Wetlands*, *34*, pp.1097-1108. https://doi.org/10.1007/s13157-014-0569-3

Veski, S., 1998. *Vegetation history, human impact and palaeogeography of West Estonia: Pollen analytical studies of lake and bog sediments* (Doctoral dissertation, Societas Upsaliensis pro geologia quaternaria [Kvartärgeologiska fören.]).

Veski, S., Koppel, K. and Poska, A., 2005. Integrated palaeoecological and historical data in the service of fine-resolution land use and ecological change assessment during the last 1000 years in Rõuge, southern Estonia. *J. of Biogeog 32*(8), pp.1473-1488. https://doi.org/10.1111/j.1365-2699.2005.01290.x

Wagner, K.I., Gallagher, S.K., Hayes, M., Lawrence, B.A. and Zedler, J.B., 2008. Wetland restoration in the new millennium: do research efforts match opportunities?. *Restor. Ecol. 16*(3), pp.367-372. https://doi.org/10.1111/j.1526-100X.2008.00433.x

Wardenaar, E.C.P., 1987. A new hand tool for cutting peat profiles. *Canadian J. of Botany*, *65*(8), pp.1772-1773. https://doi.org/10.1139/b87-243

Warner, B.G. and Asada, T., 2006. Biological diversity of peatlands in Canada. *Aquatic Sci.*, *68*, pp.240-253. https://doi.org/10.1007/s00027-006-0853-2

Waters, C.N., Turner, S.D., Zalasiewicz, J., Head, M.J., 2023. Candidate sites and other reference sections for the Global boundary Stratotype Section and Point of the Anthropocene series. *Anthropocene Rev.* https://doi.org/10.1177/20530196221136422

https://doi.org/10.5194/egusphere-2025-1351
Preprint. Discussion started: 17 April 2025

Yang, Q., Liu, Z. and Bai, E., 2023. Comparison of carbon and nitrogen accumulation rate between bog and fen phases in a pristine peatland with the fen-bog transition. *Glob. Change Biol. 29*(22), pp.6350-6366. https://doi.org/10.1111/gcb.16915

Young, D.M., Baird, A.J., Charman, D.J., Evans, C.D., Gallego-Sala, A.V., Gill, P.J., Hughes, P.D., Morris, P.J. and Swindles, G.T., 2019. Misinterpreting carbon accumulation rates in records from near-surface peat. *Sci. Rep. 9*(1), p.17939. https://doi.org/10.1038/s41598-019-53879-8

Young, D.M., Baird, A.J., Gallego-Sala, A.V. and Loisel, J., 2021. A cautionary tale about using the apparent carbon accumulation rate (aCAR) obtained from peat cores. *Sci. Rep*, *11*(1), p.9547. https://doi.org/10.1038/s41598-021-88766-8

Yu, Z., Loisel, J., Brosseau, D.P., Beilman, D.W. and Hunt, S.J., 2010. Global peatland dynamics since the Last Glacial Maximum. *Geophys. Res. Lett., 37*(13). https://doi.org/10.1029/2010GL043584

Yu, Z.C., 2012. Northern peatland carbon stocks and dynamics: a review. *Biogeosciences*, *9*(10), pp.4071-4085. https://doi.org/10.5194/bg-9-4071-2012

Zverev, V.E., Zvereva, E.L. and Kozlov, M.V., 2008b. Slow growth of Empetrum nigrum in industrial barrens: Combined effect of pollution and age of extant plants. *Env. Poll*, *156*(2), pp.454-460. https://doi.org/10.1016/j.envpol.2008.01.025

Zvereva, E.L., Toivonen, E. and Kozlov, M.V., 2008a. Changes in species richness of vascular plants under the impact of air pollution: a global perspective. *Glob. Ecol. and Biogeog. 17*(3), pp.305-319. https://doi.org/10.1111/j.1466-8238.2007.00366.x